



Grenvillian remnants in the Northern Andes: Rodinian and Phanerozoic paleogeographic perspectives

A. Cardona^{a,*}, D. Chew^b, V.A. Valencia^c, G. Bayona^d, A. Mišković^e, M. Ibañez-Mejía^c

^a Smithsonian Tropical Research Institute, Balboa, Ancón, Panama

^b Department of Geology, Trinity College Dublin, Ireland

^c Department of Geosciences, University of Arizona, Tucson, United States

^d Corporación Geológica Ares, Bogotá, Colombia

^e Department of Earth, Atmospheric, and Planetary Sciences, Massachusetts Institute of Technology, USA

ARTICLE INFO

Article history:

Received 13 March 2009

Accepted 21 July 2009

Keywords:

Grenville
Northern Andes
Terrane dispersion
Paleogeography

ABSTRACT

Grenvillian crust is encountered in several basement inliers in the northern Andes of Colombia, Ecuador and Peru and is also represented as a major detrital or inherited component within Neoproterozoic to Paleozoic sedimentary and magmatic rocks. This review of the tectonic and geochronological record of the Grenvillian belt in the northern Andes suggests that these crustal segments probably formed on an active continental margin in which associated arc and back-arc magmatism evolved from ca. 1.25 to 1.16 Ga, possibly extending to as young as 1.08 Ga.

The lithostratigraphic and tectonic history of the Grenvillian belt in the northern Andes differs from that of the Sunsas belt on the southwest Amazonian Craton and from the Grenvillian belt of Eastern Laurentia. It is considered that this belt, along with similar terranes of Grenvillian age in Middle America and Mexico define a separate composite orogen which formed on the northwestern margin of the Amazonian Craton. Microcontinent accretion and interaction with the Sveconorwegian province on Baltica is a feasible tectonic scenario, in line with recent paleogeographic reconstructions of the Rodinian supercontinent. Although Phanerozoic tectonics may have redistributed some of these terranes, they are still viewed as para-autochthonous domains that remained in proximity to the margin of Amazonia. Paleogeographic data derived from Phanerozoic rocks suggest that some of the Colombian Grenvillian fragments were connected to northernmost Peru and Ecuador until the Mesozoic, whereas the Mexican terranes were attached to the Colombian margin until Pangea fragmentation in Late Triassic times.

© 2009 Elsevier Ltd. All rights reserved.

1. Introduction

Remnants of metamorphic crust of Grenvillian age within the Andean chain (Fig. 1) are key tracers of continental interactions on the western margin of the Amazonian Craton during the Late Mesoproterozoic assembly of the supercontinent of Rodinia (Kroonenberg, 1982; Hoffman, 1991; Wasteneys et al., 1995; Kay et al., 1996; Restrepo-Pace et al., 1997; Loewy et al., 2004; Cordani et al., 2005). The Neoproterozoic to Early Paleozoic opening of the Iapetus-Tornquist and Rheic oceans, subsequent Paleozoic orogenesis and terrane accretion along with younger Meso-Cenozoic Pacific and Caribbean plate interactions have redistributed and transferred these fragments between continental masses (Ramos and Basei, 1997; Keppe and Ramos, 1999; Cawood et al., 2001; Cawood, 2005; Cardona-Molina et al., 2006; Ordóñez-Carmona et al., 2006; Chew et al.,

2008). Within the eastern Colombian Andes, high-grade, ca. 1.0–1.1 Ga metamorphic domains are discontinuously exposed along the eastern segment of the chain (Fig. 2A). Pioneering work by Kroonenberg (1982) considered this belt to represent the remnants of Grenvillian interaction between Laurentia and Amazonia. More recent geological and geochronological results have refined the paleogeographic context and tectonic implications of these basement inliers (Restrepo-Pace et al., 1997; Ruiz et al., 1999; Cordani et al., 2005; Jiménez-Mejía et al., 2006; Ordóñez-Carmona et al., 2006). In Northern Peru and Ecuador (Fig. 2B), evidence for Grenvillian crust is more limited due to extensive Phanerozoic orogenesis and sedimentary cover. However recent studies on the magmatic evolution and the provenance of the Paleozoic metamorphic complexes of the Eastern Cordilleras of Peru (north of 10 °S) and Ecuador have shown that they are derived from source regions which exhibit a major Grenvillian crustal component (Chew et al., 2007a,b, 2008; Cardona et al., 2009; Mišković et al., 2009).

In this contribution we review the published geological and geochronological record of the Mesoproterozoic domains within

* Corresponding author. Address: Smithsonian Tropical Research Institute, Center for Tropical Paleoecology and Archeology, Balboa, Ancón, Panama.

E-mail address: Cardona@si.edu (A. Cardona).

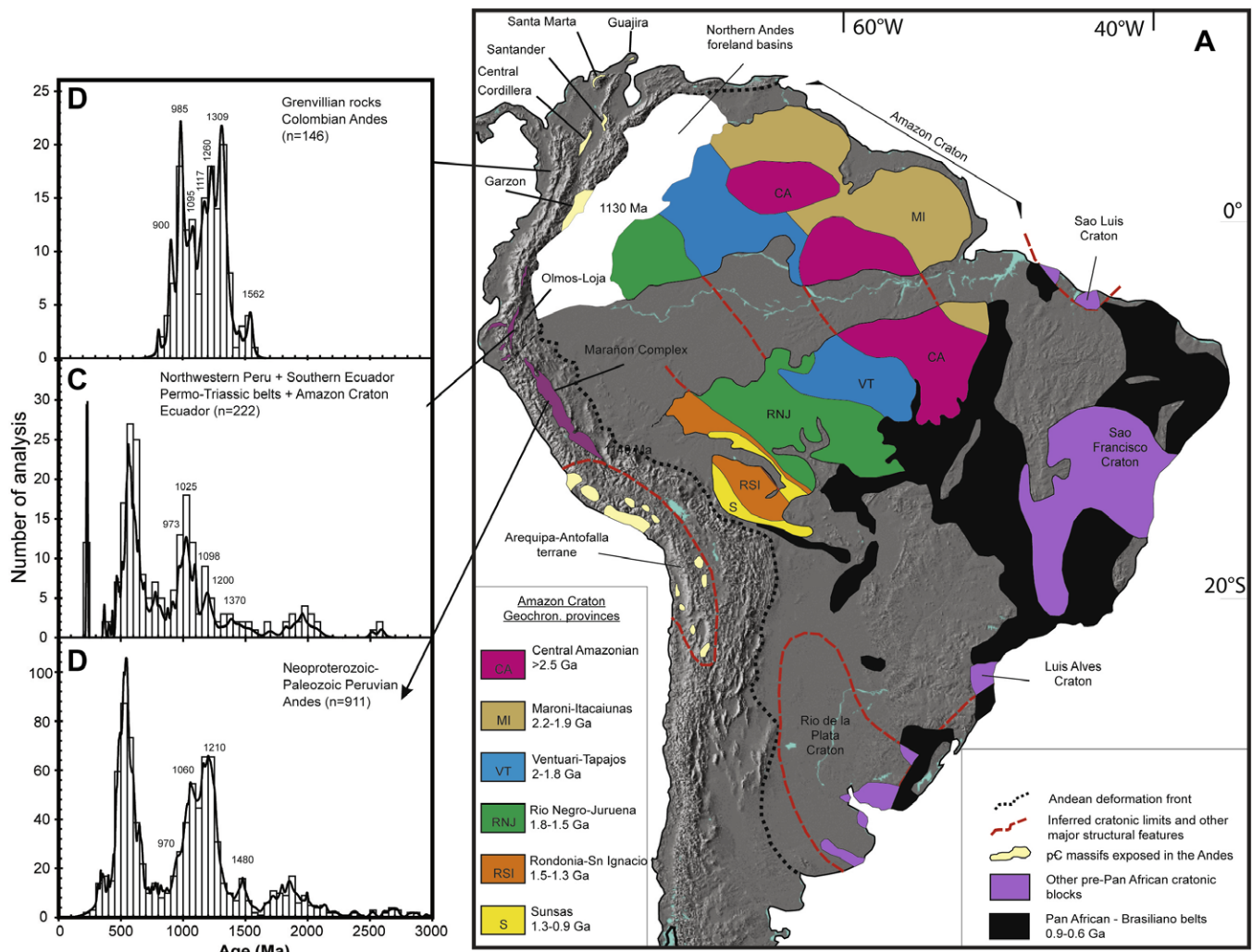


Fig. 1. Regional geological map of South America displaying the principal tectonic features of the “South American platform”. Geochronological provinces of the Amazonian Craton and Andean pre-Mesozoic inliers are modified from Cordani et al. (2000). Squares shows zircon U–Pb age distribution plots from Northern Peru, Ecuador and Colombia with particular emphasis on Grenvillian crust (database from Cordani et al. (2005), Chew et al. (2007a,b, 2008), Cardona et al. (2009), and Mišković et al. (2009)).

the Colombian Andes together with the more fragmental evidence from the Peruvian and Ecuadorian Andes (north of 10 °S). Additional new U–Pb results from a Grenvillian paragneiss from the Santa Marta Massif in northern Colombia and two Paleozoic metasediments from the northern segment of the Eastern Cordillera of Peru are presented to refine the proposed regional tectonic model. This review, when integrated with more recent constraints on the Phanerozoic paleogeography, provides new insights on the paleogeography of Rodinia and the western Amazonian Craton along this segment of the proto-Andean margin.

2. Basement inliers on the Amazonian Craton

The presence of cratonic basement in Colombia, Ecuador, Peru and Venezuela is mostly inferred as it is covered by the extensive Andean Meso-Cenozoic foreland (Fig. 1). Some windows on topographic highs along with deep oil wells have demonstrated the presence of a major crystalline basement province in Eastern Colombia (Pinson et al., 1962; Priem et al., 1982; Toussaint, 1993). However the available geochronological database is limited. Available data from exposed basement of the Amazonian Craton in Colombia include biotite K–Ar and Rb–Sr ages of ca. 1130 Ma from mylonites in the Guaviare region (Fig. 1, Pinson et al., 1962). Far-

ther east, closed to the Orinoco River and Venezuela border, U–Pb TIMS zircon and Rb–Sr data have been obtained from granitic and gneissic rocks (Priem et al., 1982). These results have been interpreted in terms of a ca. 1.5 Ga tectonomagmatic event that remobilized older 1.8 Ga crust. The ages also correlate with the Rio Negro-Juruena and Venturi Tapajos provinces of the Amazonian Craton (Tassinari et al., 2000), providing evidence for the continuity of similar basement provinces into Colombia and demonstrating the absence of Grenvillian overprint in these regions.

In Venezuela, the extent of Proterozoic basement is poorly constrained. Oil wells in the Llanos basin have sampled gneissic and granitic rocks which have yielded K–Ar biotite ages of between 1.0–1.1 Ga (2), 1.26–1.5 Ga (4) and 1.7–1.9 Ga (2) (Feo-Codoceido et al., 1984). However, K–Ar dating of K-feldspar from the same basement rocks in the Llanos basin yields Grenvillian ages, although it should be noted that the K–Ar K-feldspar system has a very low closure temperature.

A similar picture emerges from Peru and Ecuador north of 10 °S. Proterozoic rocks have been found in the Amazon Basin within the Rio Picharí region (Fig. 2B), east of Cuzco. Dalmayrac et al. (1988) reports a U–Pb zircon multigrain TIMS lower intercept age of ca. 1160 Ma from granulite-facies rocks in this region. Within the Andean foreland in Ecuador, several oil wells have sampled Late

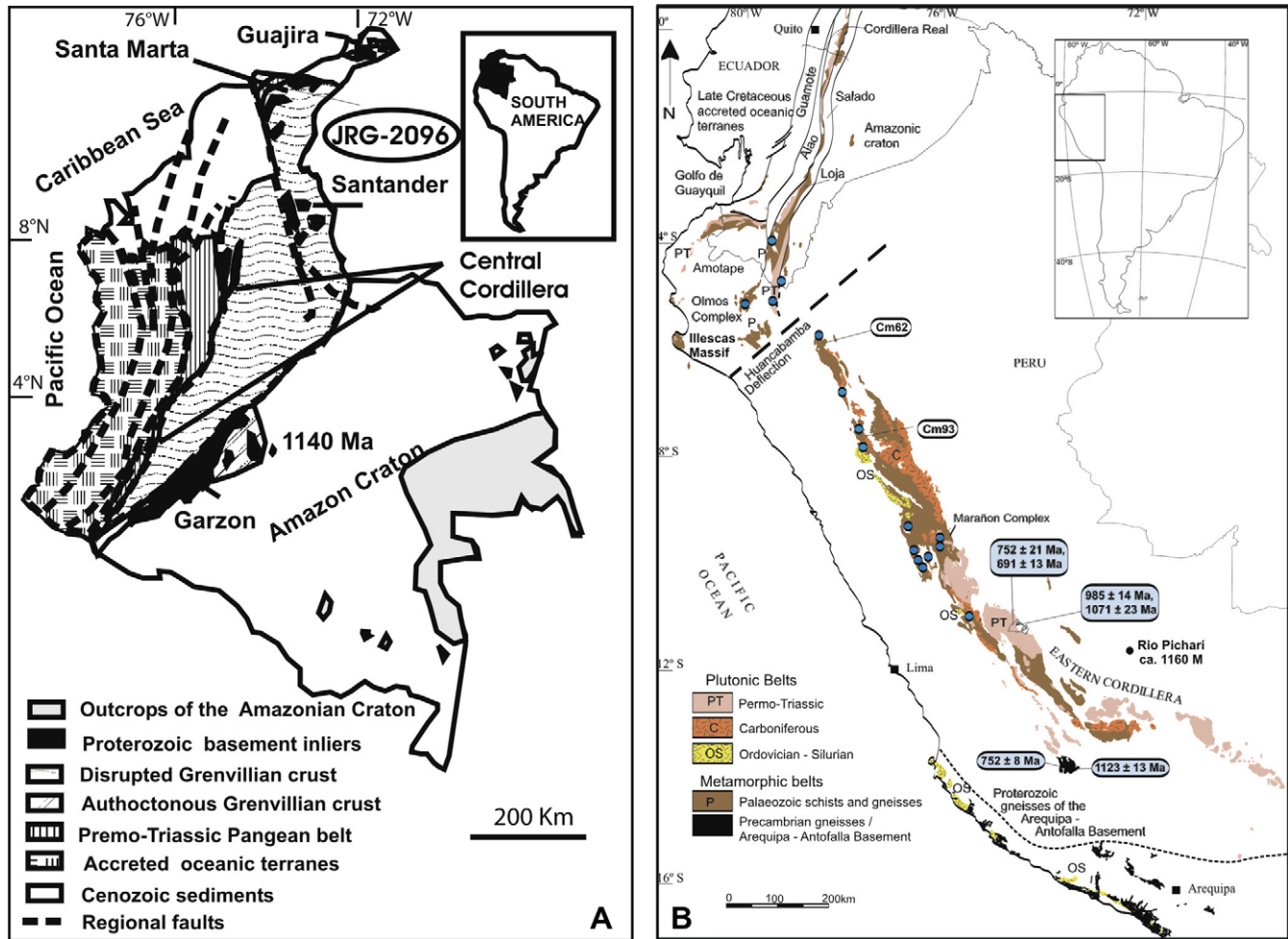


Fig. 2. (A) Terrane map of the Colombian Andes adapted from Toussaint (1993). Inliers: GC: Garzón Complex, BG: Bucaramanga Gneiss, DG: Dibuya Gneiss and LM: Los Mangos Granulite (Santa Marta region), JG: Jojoncito Gneiss (Guajira region). (B) Geological map of the Eastern Cordillera of Peru and the Eastern Cordillera and El Oro Complex of Ecuador (from Chew et al. (2008)). Older Neoproterozoic to Mesoproterozoic ages from Miškovic et al. (2009).

Mesoproterozoic basement, although the amount of published information is limited (Litherland et al., 1994). Recently, Chew et al. (2007a,b, 2008) have analyzed detrital zircons from the Isimanchi unit which forms part of the Amazonian cratonic cover in Ecuador. It consists of very low-grade phyllites and marbles and has a poorly constrained Carboniferous – Late Triassic age based on fish remains (Litherland et al., 1994). The detrital zircon distribution shows several Late Mesoproterozoic peaks at 930, 1040 and 1200 Ma (Chew et al., 2007a,b), that reinforces the presence of Grenvillian-type crust east of the Andean belt.

3. Basement inliers within the Andean belt

The most extensive remnants of Grenvillian crust within the Northern Andes are found within the Colombian Andes (Fig. 2A). Evidence from other segments of the Andean belt in Venezuela, Ecuador and Peru is more limited.

4. Colombian and Venezuelan Andes

Grenvillian high-grade metamorphic inliers have been recognized along the eastern segment of the Colombian Andes and in several massifs exposed within the Caribbean region (Fig. 2A). These inliers can be divided in two main groups: (1) the Garzón

Massif, which based on regional stratigraphic relationships with Cambrian and Jurassic rocks is considered as an autochthonous element of the northwestern Amazonian margin since Grenvillian times (Toussaint, 1993; Ordóñez-Carmona et al., 2006); (2) other Grenvillian blocks including the Santa Marta Massif, the Guajira Peninsula, the Santander Massif and the Grenvillian inliers on the eastern flank of the Central Cordillera (Toussaint, 1993; Ordóñez-Carmona et al., 2006). They are believed to represent a single terrane based on the presence of a similar Early to Middle Paleozoic tectonomagmatic overprint. Although other authors have preferred an autochthonous origin for these rocks (e.g. Restrepo-Pace et al., 1997; Cedié et al., 2003), we favor a para-autochthonous origin for these domains.

Grenvillian crust has not yet been documented within the Venezuelan Andes. However, the presence of inherited zircons within Neoproterozoic – Early Paleozoic granitoids argue for the assimilation of older (ca. 1.0 Ga) crust (Burkley, 1976). Zircons from recent sands from the Orinoco River show a strong Mesoproterozoic Grenvillian signature between 1.0 and 1.4 Ga (Goldstein et al., 1997). Much of this sand probably originated in Eastern Colombian and the Venezuelan Andes (Johnson, 1991). The K'Mudku belt which is an eastern intraplate expression of Grenvillian tectonics, may have also contributed to the sediment budget of the Orinoco River (Santos et al., 2008), however the understanding of the geological evolution of this belt is still limited.

4.1. Garzón Massif

The Garzón Massif is the best exposed portion of Grenvillian crust in the Colombian Andes. It is divided into three main lithostratigraphic units (reviews in Kroonenberg, 1982; Jiménez-Mejía et al., 2006). (1) The Guapotón-Moncagua Orthogneiss which comprises predominantly hornblende-biotite augen gneisses. (2) The El Vergel Granulites which are comprised of quartzfeldspathic gneisses, charnockite to enderbite garnet granulites, and intercalations of mafic, ultramafic and calc-silicate rocks. $P-T$ determinations suggest a counterclockwise $P-T$ path, with metamorphic conditions that range between 5.3–6.2 kbar and 700–780 °C and 6.2–7.2 kbar and 685–740 °C (Jiménez-Mejía et al., 2006). (3) The Las Margaritas Gneiss is composed of banded biotite-garnet sillimanite gneisses and migmatites, with discordant granitic leucosomes and local high temperature mylonitic zones. The geothermobarometric data define a clockwise $P-T$ path, with pressures between 6.3 and 8.8 kbar and temperatures of 680–820 °C. These two units have been considered as part of a metamorphosed volcano-sedimentary sequence (Kroonenberg, 1982, 2001).

Recent reviews on the geochronology of the Garzón Massif by Restrepo-Pace et al. (1997) and Cordani et al. (2005) together with previous Rb-Sr and K-Ar data (Priem et al., 1989) clearly indicate a prolonged tectonic history from ca. 1180 to 915 Ma.

Single grain SHRIMP U-Pb zircon geochronology from the Guapotón Gneiss yields a 1158 ± 23 Ma age for the magmatic precursor (Cordani et al., 2005). This age is similar to a former TIMS age presented by Restrepo-Pace et al. (1997). A younger 1000 ± 25 Ma zircon overgrowth reflects subsequent high-grade metamorphism (Cordani et al., 2005). A discordant migmatitic leucosome from the Las Margaritas Gneiss yields a U-Pb SHRIMP age of 1015 ± 8 Ma, whereas Sm-Nd garnet-whole rock isochrons from two high-grade gneisses yield ages of 1034 ± 6 Ma and 990 ± 8 Ma (Cordani et al., 2005). A sample from the Vergel Granulites has yielded similar SHRIMP U-Pb ages of ca. 1000 Ma which are interpreted as recording metamorphic crystallization, whereas Sm-Nd garnet-whole rock isochrons show ages of 935 ± 5 Ma and 925 ± 7 Ma.

4.2. Santander Massif

The Bucaramanga gneiss represents the major Precambrian basement unit in the Santander Massif (Fig. 2A). It is comprised of a metasedimentary sequence of sillimanite, cordierite and garnet paragneisses, with intercalations of marble, calc-silicate rock and minor amphibolite (Ward et al., 1973).

Local tonalitic to granitic leucosomes are related to partial melting. Plagioclase-hornblende thermobarometry in a biotite-amphibole gneiss yield pressures of 4–6 kbar and temperatures between 600 and 800 °C (Cardona, 2003). U-Pb zircon SHRIMP results include inherited zircons between 1.5 and 1.04 Ga related to the detrital protolith, whereas the youngest zircon ages of 864 ± 66 Ma within a zircon overgrowth is related to a late metamorphic event (Cordani et al., 2005). Ar-Ar mineral dating of amphibole and biotite are reset by a major Jurassic tectono-magmatic event of regional extent (Restrepo-Pace et al., 1997; Cordani et al., 2005). Ward et al. (1973) report a K-Ar hornblende cooling age of 945 ± 40 Ma in another segment of the massif.

4.3. Santa Marta Massif and Guajira region

In the Santa Marta Massif (Fig. 2A), high-grade, amphibolite to granulite-facies metamorphic rocks have been documented within the Los Mangos Granulite and Dibuya Gneiss (MacDonald and Hurley, 1969; Tschanz et al., 1974). These rocks are intruded and segmented by Jurassic magmatic rocks (Tschanz et al., 1974). Compositinally they include banded felsic and intermediate

gneiss, pelitic paragneiss, hornblende-pyroxene gneiss and calc-silicate rock along with metamorphosed anorthositic stocks and dykes (Tschanz et al., 1974).

Amphibole thermobarometry from the Dibuya Gneiss has yielded $P-T$ conditions of 6.0–7.6 kbar and 760–810 °C (Cardona-Molina et al., 2006). Geochemical data from amphibolites on the northeastern segment of the Santa Marta Massif have suggested a rift-related origin, probably linked to a back-arc setting (Cardona-Molina et al., 2006). The presence of anorthosite bodies may be related to this extensional setting or possibly to lithospheric thinning following orogenic collapse (Ashwal, 1993; Gower and Krogh, 2002).

U-Pb zircon ages between ca. 1500 and 980 Ma were obtained by Restrepo-Pace et al. (1997) and Cordani et al. (2005). The older ages are related to cores from detrital sedimentary protolith (Ordóñez-Carmona et al., 2002, 2006), while the youngest age of 993 ± 12 Ma in a zircon rim is thought to be related to a late metamorphic event.

A Sm-Nd garnet isochron from a granulite yields an age of 971 ± 8 Ma (Ordóñez-Carmona et al., 2006), whereas K/Ar and Ar-Ar hornblende ages of 930 Ma reflect Subsequent cooling (Tschanz et al., 1974; Cordani et al., 2005).

We have analyzed 58 zircon grains from a paragneiss sample (JRG-20-96) from the Los Mangos Granulite on the eastern flank of the Sierra Nevada de Santa Marta (Fig. 3A). The obtained U-Pb ages range mainly from the Middle to Late Mesoproterozoic, between 996 and 1372 Ma. Three major age peaks at 1025, 1235 and 1315 Ma are recognized. These ages are related to the sources of the sedimentary protolith. The Jojoncito Gneiss, a fine- to medium grained paragneiss, crops out in the Guajira region in northeastern Colombia. Pb- α and U-Pb SHRIMP geochronology (Banks, 1975; Cordani et al., 2005) records a polymetamorphic evolution with a major metamorphic event at ca. 915 Ma and evidence of an older event at ca. 1165 Ma. Older ages between 1220 and 1570 Ma are related to detrital material that forms the protolith. Other evidence of Grenvillian crust in the Caribbean region includes displaced blocks in Bonaire, Leeward Antilles, where gneissic boulders found in an Eocene conglomerate have yielded U-Pb zircon ages of ca. 1160 Ma (Priem et al., 1986). Clasts from the Oligocene Falcón basin and the coastal complexes of Venezuela include high-grade metamorphic rocks that have been attributed to Grenvillian basement (Grande et al., 2007).

4.4. Eastern flank of the Central Cordillera

Along the eastern segment of the Central Cordillera and in the adjacent northern San Lucas Serranía (Fig. 2A), several high-grade amphibolite-facies and probable granulite-facies rocks are considered to have undergone metamorphism during Grenvillian times (Toussaint, 1993; Ordoñez-Carmona et al., 1999; Ordóñez-Carmona et al., 2007). Mylonitic gneisses in the northern segment of the cordillera have yielded a Rb-Sr isochron age of 894 ± 36 Ma (Ordoñez-Carmona et al., 1999), which they relate to the main mylonitic event affecting these rocks. Further south, amphibolite-facies rocks which are unconformably overlain by Ordovician sediments have yielded Ar-Ar amphibole cooling ages of 911 ± 2 Ma (Restrepo-Pace et al., 1997). Vesga and Barrero (1978) report a K-Ar amphibole age of ca. 1.3 Ga from a similar amphibolite further north in the region.

5. Eastern Cordillera of Peru

Classic exposures of Grenvillian crust crop out in the Arequipa Massif of southeastern Peru, where Paleoproterozoic crust was reworked during the 1.0–1.2 Ga Grenvillian event (Wasteneys et al., 1995; Loewy et al., 2004).

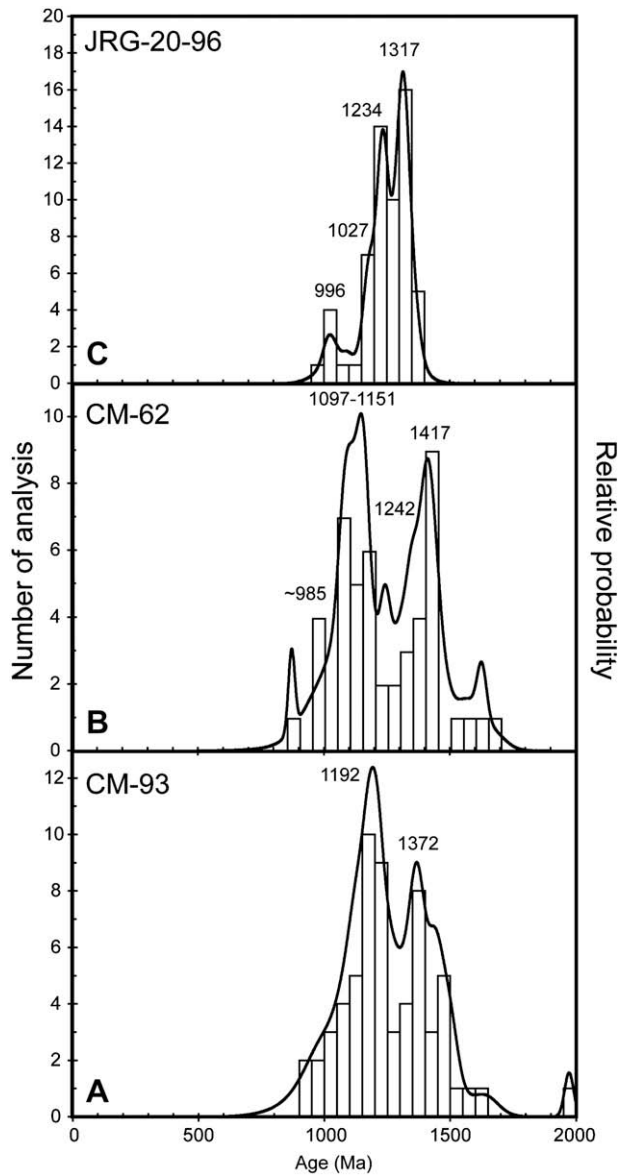


Fig. 3. U-Pb detrital zircon ages of the analyzed samples from the Colombian and Peruvian Andes.

North of Lima, pre-Mesozoic metasedimentary basement crops out extensively in the Eastern Cordillera, where it is termed the Marañon Complex (Fig. 2B; Wilson and Reyes, 1964). Additionally, there are remnants of metamorphic basement of unknown age in the coastal and offshore regions of Peru (Thornburg and Kulum, 1981; Ramos, 2008).

Recent studies dealing with the geological and geochronological evolution of the Eastern Cordillera have shown that it mainly consists of different units of Paleozoic age (Cardona et al., 2007, 2009; Chew et al., 2007a,b, 2008; Miškovic et al., 2009). However, minor remnants of Neoproterozoic and Late Mesoproterozoic crystalline basement are also exposed (Cardona et al., 2009; Miškovic et al., 2009).

The tectonic evolution of the Eastern Cordillera during the Paleozoic is linked to tectonic processes that include either continuous ocean-continent convergence, or to a series of periods of arc magmatism interrupted by terrane accretionary events (Chew et al., 2007a,b; Ramos, 2008; Cardona et al., 2009; Miškovic et al., 2009).

The presence of Grenvillian crust is restricted to partially foliated and compositionally diverse granitoids from the south-central cordilleran segment which have yielded U-Pb zircon crystallization ages of 985 ± 14 Ma, 1071 ± 23 Ma to 1123 ± 23 Ma (Miškovic et al., 2009). Additional insights on the nature of the Grenvillian event on this sector of the proto-Andean margin are provided by the detrital and inherited U-Pb zircon signature of the Paleozoic sedimentary and magmatic record (Chew et al., 2007a,b, 2008; Cardona et al., 2009). The published U-Pb detrital zircon data show the existence of a major Mesoproterozoic Grenvillian source, and age populations are apparently coherent along most of the Paleozoic units of the Eastern Cordillera of Peru. The homogeneity in the observed age populations suggests that if terrane accretion did influence the Paleozoic tectonics of the Peruvian margin, then these terranes probably share a common origin, probably as para-autochthonous terranes (Ramos and Basei, 1997; Ramos, 2008; Cardona et al., 2009). Two additional samples from the northern region have been incorporated in this study to complement this database. Sample CM-93 was collected from a pre-Carboniferous meta-arenite from the Pataz region (Fig. 3A). Sixty-six zircons from this sample were analyzed by the U-Pb LA-MC-ICP-MS method at the LASERCHRON laboratory in Arizona (analytical technique is presented in the Appendix 1). Zircons are typically prismatic with rounded tips, and most analyses are concordant. All zircons have U/Th ratios lower than 12, and therefore are most likely related to sources derived from magmatic rocks (Rubatto, 2002). The youngest U-Pb zircon age is 522 ± 5 Ma whereas the oldest is 1640 ± 49 Ma (Table 1, appendix). However, the majority of the $^{206}\text{Pb}/^{238}\text{U}$ ages ($n = 61$) extend between 962 ± 27 and 1433 ± 29 Ma, with major peaks at 1192 and 1372 Ma (Fig. 3B). Another sample (CM-62) was collected from another pre-Carboniferous meta-arenite exposed further north close to the Kuelap archeological site (Fig. 2B). Forty-six subrounded to prismatic zircons were analyzed, and most of them yield concordant ages which extend between 900 and 1700 Ma (Fig. 3B), with three major age distribution peaks at 1150, 1240 and 1417 Ma. By combining the entire detrital and inherited zircon ages from the Eastern Peruvian Andes, major Mesoproterozoic age distribution peaks are encountered at 970, 1060, 1210 and 1480 Ma (Fig. 1B).

6. Ecuador and northwestern Peru

In Ecuador and northwestern Peru in the vicinity of the Huancahuambla deflection, basement rocks comprise the low-grade metamorphic rocks of the Olmos Complex and the Triassic syn-tectonic granitoids and amphibolites of the Illescas, Paita and the Amotape Mountains (Figs. 1a and 2b, Noble et al., 1997; Vinasco, 2004; Chew et al., 2007a,b; Cardona et al., 2008). These elements are grouped into a composite regional lithostratigraphic entity that extends toward the Cordillera Real and the El Oro belt of Ecuador. The core and the western flank of the Central Cordillera of Colombia is composed of metamorphic rocks of the same probable tectonic affinity (Toussaint, 1993; Litherland et al., 1994; Noble et al., 1997; Vinasco et al., 2006). The origin of this dismembered terrane is related to accretionary tectonics associated with the closure of the Rheic ocean (Rowley and Pindell, 1989; Toussaint, 1993; Vinasco et al., 2006; Nance and Linnemann, 2008). Some authors have proposed a para-autochthonous origin for this terrane (Noble et al., 1997; Pratt et al., 2005), which is corroborated by similarities between the detrital zircon signature of the Late Paleozoic cover sequences on the Amazonian Craton and the para-autochthonous sequences to the west (Chew et al., 2007a,b). The detrital signature from several Late Paleozoic samples from the Olmos Complex of Peru, the El Oro belt of Ecuador and the

Table 1

U-Pb zircon LA-MC-ICP-MS analytical results.

Analysis	U (ppm)	206Pb 204Pb	U/Th	207Pb [*] 235U [*]	± (%)	206Pb [*] 238U	± (%)	error corr.	206Pb [*] 238U [*]	± (Ma)	207Pb [*] 235U	± (Ma)	206Pb [*] 207Pb [*]	± (Ma)	Best age (Ma)	± (Ma)
JRG2096-1	593	135,655	5.0	2.1799	1.4	0.1992	1.0	0.71	1171.0	10.7	1174.7	9.8	1181.3	19.8	1181.3	19.8
JRG2096-2	542	101,100	5.1	2.1428	1.9	0.1957	1.6	0.85	1152.3	17.3	1162.7	13.3	1182.2	19.8	1182.2	19.8
JRG2096-3	419	92,045	4.5	2.2109	1.4	0.2021	1.0	0.71	1186.6	10.8	1184.5	9.9	1180.6	19.8	1180.6	19.8
JRG2096-4	423	114,595	3.7	2.8197	1.5	0.2390	1.1	0.73	1381.3	13.2	1360.8	10.9	1328.7	19.4	1328.7	19.4
JRG2096-5	402	124,260	6.3	2.2737	1.5	0.2021	1.2	0.76	1186.4	12.7	1204.2	10.9	1236.1	19.6	1236.1	19.6
JRG2096-6	399	79,140	4.7	2.4703	1.4	0.2181	1.0	0.71	1272.0	11.5	1263.4	10.2	1248.6	19.6	1248.6	19.6
JRG2096-7	801	179,250	5.8	2.6931	1.4	0.2286	1.0	0.71	1327.1	12.0	1326.6	10.5	1325.7	19.4	1325.7	19.4
JRG2096-8	209	39,725	4.3	1.6961	1.8	0.1660	1.4	0.75	989.8	12.6	1007.1	11.7	1044.7	24.6	1044.7	24.6
JRG2096-10	110	30,325	4.7	2.5962	2.2	0.2205	1.6	0.70	1284.7	18.3	1299.6	16.4	1324.2	30.8	1324.2	30.8
JRG2096-11	666	152,965	5.4	2.4839	2.0	0.2136	1.7	0.85	1248.2	19.1	1267.4	14.3	1300.1	20.0	1300.1	20.0
JRG2096-12	415	159,630	5.7	2.6845	1.4	0.2284	1.0	0.71	1326.3	12.0	1324.2	10.5	1320.7	19.4	1320.7	19.4
JRG2096-13	763	220,075	7.3	2.4527	2.0	0.2121	1.8	0.87	1240.2	20.0	1258.2	14.7	1289.2	19.5	1289.2	19.5
JRG2096-14	231	74,900	4.7	2.5462	1.9	0.2196	1.3	0.69	1279.9	15.6	1285.3	14.2	1294.4	27.4	1294.4	27.4
JRG2096-15	678	83,370	4.5	2.4364	1.8	0.2119	1.6	0.84	1238.9	17.5	1253.4	13.3	1278.4	19.5	1278.4	19.5
JRG2096-16	638	159,045	7.1	2.5161	2.5	0.2155	2.3	0.91	1257.8	25.7	1276.7	17.9	1308.6	19.4	1308.6	19.4
JRG2096-17	152	41,090	4.3	2.6085	1.4	0.2229	1.0	0.71	1297.0	11.7	1303.0	10.4	1313.0	19.4	1313.0	19.4
JRG2096-18	366	65,560	7.9	2.0965	1.4	0.1860	1.0	0.71	1099.4	10.1	1147.7	9.7	1240.0	19.6	1240.0	19.6
JRG2096-19	99	20,780	0.8	1.6626	3.9	0.1666	2.9	0.75	993.5	27.1	994.4	24.9	996.3	52.9	996.3	52.9
JRG2096-20	503	78,875	5.1	2.1937	1.9	0.1960	1.6	0.85	1153.8	17.0	1179.0	13.3	1225.6	19.8	1225.6	19.8
JRG2096-21	378	61,795	3.1	2.6630	2.3	0.2228	2.1	0.90	1296.7	24.8	1318.2	17.2	1353.5	19.3	1353.5	19.3
JRG2096-22	323	55,600	4.0	2.1554	9.1	0.1891	6.8	0.75	1116.7	70.0	1166.8	63.0	1261.1	116.6	1261.1	116.6
JRG2096-23	185	40,510	4.0	2.3492	3.1	0.2075	2.9	0.93	1215.5	32.0	1227.3	22.2	1248.2	23.1	1248.2	23.1
JRG2096-24	384	108,150	5.8	2.5484	1.4	0.2174	1.0	0.71	1268.2	11.5	1286.0	10.3	1315.8	19.4	1315.8	19.4
JRG2096-25	581	241,380	6.7	2.4831	1.8	0.2144	1.5	0.83	1252.5	16.7	1267.1	12.9	1292.0	19.5	1292.0	19.5
JRG2096-26	695	242,840	6.2	2.5872	1.5	0.2196	1.1	0.75	1279.9	13.0	1297.0	11.0	1325.4	19.4	1325.4	19.4
JRG2096-26A	614	174,960	48.7	1.8512	1.6	0.1728	1.1	0.71	1027.5	10.5	1063.9	10.3	1139.2	22.1	1139.2	22.1
JRG2096-27	393	164,215	7.9	2.2273	1.4	0.1979	1.0	0.70	1164.3	10.7	1189.7	10.0	1236.2	20.0	1236.2	20.0
JRG2096-28	166	75,640	9.8	2.4688	3.5	0.2126	2.3	0.65	1242.9	26.1	1262.9	25.5	1297.2	51.9	1297.2	51.9
JRG2096-29	421	108,690	8.5	1.5534	3.1	0.1533	2.6	0.85	919.5	22.6	951.9	19.3	1027.3	33.8	1027.3	33.8
JRG2096-30	673	220,680	7.8	2.3322	2.4	0.2048	1.9	0.76	1201.2	20.4	1222.2	17.3	1259.4	30.7	1259.4	30.7
JRG2096-31	119	17,590	3.2	2.8039	3.4	0.2347	2.7	0.78	1359.2	33.1	1356.6	25.8	1352.3	41.4	1352.3	41.4
JRG2096-32	1192	91,980	5.1	1.7795	1.9	0.1699	1.6	0.85	1011.6	14.9	1038.0	12.2	1093.9	20.0	1093.9	20.0
JRG2096-33	854	110,870	3.5	2.1477	1.9	0.1969	1.7	0.86	1158.5	17.5	1164.3	13.4	1175.1	19.8	1175.1	19.8
JRG2096-34	147	43,570	4.5	2.2784	3.3	0.2014	2.5	0.76	1182.8	27.2	1205.6	23.4	1246.8	42.3	1246.8	42.3
JRG2096-36	478	88,815	3.8	2.4840	2.0	0.2120	1.7	0.86	1239.6	19.3	1267.4	14.3	1314.8	19.4	1314.8	19.4
JRG2096-37	306	61,575	4.4	2.3068	1.6	0.2060	1.0	0.63	1207.2	11.0	1214.4	11.2	1227.2	24.0	1227.2	24.0
JRG2096-38	684	132,900	4.3	2.6916	2.8	0.2268	2.6	0.93	1317.5	30.7	1326.1	20.5	1340.1	19.3	1340.1	19.3
JRG2096-39	580	72,210	3.8	1.6300	3.3	0.1599	1.0	0.31	956.1	8.9	981.9	20.6	1039.8	62.8	1039.8	62.8
JRG2096-40	486	67,625	3.6	2.2941	1.7	0.2048	1.0	0.60	1201.0	11.0	1210.5	11.7	1227.3	25.9	1227.3	25.9
JRG2096-35	609	141,520	4.0	2.1153	1.4	0.1946	1.0	0.71	1146.2	10.5	1153.8	9.8	1168.0	19.8	1168.0	19.8
JRG2096-41	612	96,570	2.6	2.4449	1.5	0.2155	1.2	0.75	1257.8	13.1	1255.9	11.0	1252.6	19.6	1252.6	19.6
JRG2096-42	646	100,735	3.4	2.5550	2.7	0.2185	2.6	0.93	1274.0	29.5	1287.9	20.0	1311.1	19.4	1311.1	19.4
JRG2096-43	379	53,780	4.4	1.6931	1.4	0.1681	1.0	0.71	1001.7	9.3	1005.9	9.0	1015.2	20.3	1015.2	20.3
JRG2096-44	281	34,970	2.7	2.7113	1.4	0.2271	1.0	0.70	1319.3	11.9	1331.6	10.5	1351.4	19.5	1351.4	19.5
JRG2096-45	290	28,100	3.9	2.8287	2.3	0.2343	2.1	0.90	1357.0	25.3	1363.2	17.2	1372.8	19.2	1372.8	19.2
JRG2096-46	169	37,530	3.4	2.2996	1.9	0.2086	1.0	0.52	1221.2	11.1	1212.2	13.6	1196.1	32.4	1196.1	32.4
JRG2096-48	866	90,765	9.1	2.1397	5.9	0.1905	5.8	0.99	1124.2	59.5	1161.7	40.6	1232.4	19.8	1232.4	19.8
JRG2096-49	967	85,210	3.2	2.3152	2.6	0.2006	2.5	0.93	1178.8	26.4	1217.0	18.8	1285.3	19.5	1285.3	19.5
JRG2096-50	98	28,540	4.6	2.6053	3.6	0.2214	2.8	0.79	1289.2	33.1	1302.1	26.2	1323.4	42.0	1323.4	42.0
JRG2096-51	378	21,550	5.0	2.1275	1.6	0.1899	1.3	0.78	1120.7	12.9	1157.8	11.1	1227.9	19.9	1227.9	19.9
JRG2096-52	365	127,625	4.0	2.2150	1.4	0.1992	1.0	0.71	1171.2	10.7	1185.8	9.9	1212.5	19.7	1212.5	19.7
JRG2096-53	274	101,495	6.3	2.5357	5.3	0.2153	5.2	0.98	1257.2	58.9	1282.3	38.3	1324.7	19.4	1324.7	19.4
JRG2096-54	498	115,415	6.6	2.2685	1.6	0.2019	1.2	0.77	1185.3	13.1	1202.6	11.1	1233.6	19.6	1233.6	19.6
JRG2096-55	676	164,820	5.6	2.5842	1.5	0.2199	1.2	0.76	1281.3	13.6	1296.2	11.3	1320.8	19.4	1320.8	19.4
JRG2096-56	545	48,300	4.2	2.2709	3.9	0.1997	3.2	0.83	1173.7	34.3	1203.3	27.2	1256.7	41.9	1256.7	41.9
JRG2096-57	892	79,560	6.2	1.9422	5.1	0.1781	3.7	0.72	1056.3	35.9	1095.8	34.3	1175.0	70.5	1175.0	70.5
JRG2096-58	354	67,235	6.5	2.6361	1.8	0.2262	1.5	0.84	1314.6	18.2	1310.8	13.5	1304.4	19.4	1304.4	19.4
JRG2096-59	212	28,900	2.9	2.9276	2.6	0.2426	1.2	0.48	1400.0	15.6	1389.1	19.6	1372.3	43.8	1372.3	43.8
JRG2096-60	617	73,480	2.6	2.0720	7.0	0.1863	6.9	0.99	1101.0	70.2	1139.6	48.1	1213.7	19.7	1213.7	19.7
CM62-1	107	7169	5.0	1.90,123	5.87	0.18284	3.36	0.57	1082.5	33.5	1081.5	39.1	1080	97	1080	97
CM62-2	150	16,908	2.5	2.88842	2.56	0.23620	1.83	0.72	1366.9	22.5	1378.9	19.3	1397	34	1397	34
CM62-3	175	25,679	5.0	1.68452	3.92	0.16872	1.13	0.29	1005.1							

Table 1 (continued)

Analysis	U (ppm)	206Pb 204Pb	U/Th	207Pb* 235U*	± (%)	206Pb* 238U	± (%)	error corr.	206Pb* 238U*	± (Ma)	207Pb* 235U	± (Ma)	206Pb* 207Pb*	± (Ma)	Best age (Ma)	± (Ma)
CM62-15	530	11,008	3.1	1.75997	2.41	0.16352	2.03	0.84	976.3	18.4	1030.8	15.6	1148	26	1148	26
CM62-16	146	14,984	0.6	2.80744	3.04	0.23698	1.00	0.33	1371.0	12.4	1357.5	22.8	1336	56	1336	56
CM62-17	132	9972	1.8	2.45098	2.73	0.21191	1.07	0.39	1239.0	12.1	1257.7	19.7	1290	49	1290	49
CM62-18	302	17,352	1.9	1.87439	2.40	0.17932	1.73	0.72	1063.3	17.0	1072.1	15.9	1090	33	1090	33
CM62-19	337	17,201	1.0	2.16578	5.03	0.18118	3.76	0.75	1073.4	37.2	1170.1	35.0	1354	64	1354	64
CM62-20	206	17,620	1.9	2.05202	3.80	0.19423	2.90	0.76	1144.2	30.4	1133.0	25.9	1111	49	1111	49
CM62-21	180	47,254	1.8	2.56875	2.30	0.21983	1.76	0.77	1281.0	20.4	1291.8	16.8	1310	29	1310	29
CM62-22	64	3554	1.7	2.90531	7.17	0.23391	5.34	0.74	1355.0	65.3	1383.3	54.2	1427	91	1427	91
CM62-23	224	20,178	4.2	2.02166	1.88	0.18761	1.07	0.57	1108.4	10.9	1122.8	12.8	1151	31	1151	31
CM62-24	94	8072	2.0	2.63981	7.38	0.21530	5.35	0.72	1257.0	61.1	1311.8	54.4	1403	97	1403	97
CM62-25	31	5544	2.1	2.81301	6.43	0.23042	3.89	0.61	1336.7	47.0	1359.0	48.2	1394	98	1394	98
CM62-26	63	4787	1.7	3.23734	5.14	0.25074	1.51	0.29	1442.3	19.5	1466.1	39.9	1501	93	1501	93
CM62-27	279	21,375	1.5	2.81425	1.94	0.22789	1.00	0.51	1323.4	12.0	1359.3	14.6	1416	32	1416	32
CM62-28	103	21,367	1.7	3.10031	2.88	0.25110	2.12	0.74	1444.2	27.4	1432.8	22.1	1416	37	1416	37
CM62-29	186	19,691	3.4	1.74253	3.05	0.16947	1.83	0.60	1009.2	17.1	1024.4	19.7	1057	49	1057	49
CM62-30	74	7192	1.6	1.73173	5.31	0.16367	2.38	0.45	977.2	21.6	1020.4	34.2	1114	95	1114	95
CM62-31	474	8032	3.2	2.82359	3.42	0.20438	3.26	0.95	1198.8	35.7	1361.8	25.6	1628	19	1628	19
CM62-32	194	3986	2.0	1.75245	3.15	0.16574	1.08	0.34	988.6	9.9	1028.1	20.4	1113	59	1113	59
CM62-33	89	4122	1.9	1.62123	3.53	0.16431	1.33	0.38	980.7	12.1	978.5	22.1	973	67	973	67
CM62-34	372	17,888	4.1	2.21282	1.72	0.19603	1.00	0.58	1154.0	10.6	1185.1	12.0	1242	27	1242	27
CM62-35	360	9789	1.8	2.10884	1.76	0.19267	1.19	0.68	1135.8	12.4	1151.7	12.1	1182	26	1182	26
CM62-36	217	10,014	2.2	2.77110	4.34	0.22389	3.89	0.90	1302.4	45.9	1347.8	32.4	1421	37	1421	37
CM62-37	1238	13,334	1.7	1.78918	1.80	0.16511	1.49	0.83	985.1	13.6	1041.5	11.7	1162	20	1162	20
CM62-38	1491	29,924	6.7	1.74248	1.42	0.16826	1.00	0.71	1002.5	9.3	1024.4	9.2	1071	20	1071	20
CM62-39	434	8999	1.3	2.48227	1.57	0.20812	1.17	0.74	1218.8	13.0	1266.9	11.4	1349	20	1349	20
CM62-40	857	28,211	13.1	1.79043	1.42	0.17081	1.00	0.70	1016.6	9.4	1042.0	9.2	1096	20	1096	20
CM62-41	161	12,417	2.0	2.77358	4.14	0.22800	2.13	0.52	1324.0	25.5	1348.5	30.9	1387	68	1387	68
CM62-42	708	16,124	1.8	1.75387	1.94	0.16470	1.65	0.85	982.8	15.0	1028.6	12.5	1127	20	1127	20
CM62-43	1427	34,638	12.1	2.09493	2.69	0.19413	2.50	0.93	1143.7	26.2	1147.1	18.5	1154	20	1154	20
CM62-44	428	5234	1.7	3.04077	4.18	0.22657	3.67	0.88	1316.5	43.7	1417.9	32.0	1574	38	1574	38
CM62-45	1405	33,795	11.2	2.19255	1.42	0.19414	1.00	0.71	1143.8	10.5	1178.7	9.9	1243	20	1243	20
CM62-46	197	7513	2.2	1.97135	3.82	0.18798	1.67	0.44	1110.4	17.0	1105.8	25.7	1097	69	1097	69
CM62-47	213	10,638	1.6	2.01055	2.93	0.18504	1.00	0.34	1094.4	10.1	1119.1	19.8	1167	54	1167	54
CM93-1	706	39,850	5.4	2.12745	3.45	0.19168	3.30	0.96	1130.4	34.2	1157.8	23.8	1209	20	1209	20
CM93-2	433	28,747	2.0	3.22654	4.66	0.25145	4.38	0.94	1445.9	56.7	1463.6	36.2	1489	30	1489	30
CM93-3	265	20,508	1.4	1.78813	3.21	0.17161	2.53	0.79	1021.0	23.9	1041.1	20.9	1084	40	1084	40
CM93-4	128	29,617	1.5	5.53835	1.42	0.33181	1.00	0.71	1847.2	16.1	1906.6	12.2	1972	18	1972	18
CM93-5	862	38,874	3.2	2.70146	1.42	0.22201	1.00	0.71	1292.5	11.7	1328.9	10.5	1388	19	1388	19
CM93-6	165	9018	3.0	1.49583	5.20	0.15546	4.06	0.78	931.5	35.2	928.7	31.7	922	67	922	67
CM93-7	133	7368	1.5	1.75150	3.04	0.16926	2.10	0.69	1008.0	19.6	1027.7	19.7	1070	44	1070	44
CM93-8	1051	4027	3.9	1.03383	1.52	0.10556	1.00	0.66	646.9	6.2	720.8	7.8	958	23	647	6
CM93-9	806	3547	1.3	1.43675	4.87	0.13506	4.60	0.94	816.7	35.3	904.4	29.2	1125	32	1125	32
CM93-10	724	3777	1.2	0.86922	2.92	0.09025	1.99	0.68	557.0	10.6	635.1	13.8	924	44	557	11
CM93-11	272	12,762	2.2	2.14297	3.73	0.19823	2.11	0.57	1165.8	22.5	1162.8	25.9	1157	61	1157	61
CM93-12	264	28,080	3.2	2.12462	3.09	0.19465	2.92	0.94	1146.5	30.7	1156.8	21.3	1176	20	1176	20
CM93-13	56	3888	2.3	2.09147	4.19	0.19017	3.22	0.77	1122.3	33.2	1146.0	28.8	1191	53	1191	53
CM93-14	83	7468	1.9	1.87581	5.61	0.17315	3.82	0.68	1029.5	36.4	1072.6	37.1	1161	81	1161	81
CM93-15	31	2451	1.3	3.23168	3.82	0.25169	2.43	0.64	1447.2	31.6	1464.8	29.6	1490	56	1490	56
CM93-16	42	5396	1.4	2.27924	3.40	0.20519	2.34	0.69	1203.1	25.7	1205.9	24.0	1211	48	1211	48
CM93-17														44		44
CM93-18	86	10,842	2.4	2.68480	4.20	0.22927	1.88	0.45	1330.7	22.6	1324.3	31.1	1314	73	1314	73
CM93-19	121	16,032	1.7	2.50959	2.62	0.21830	1.14	0.44	1272.9	13.2	1274.8	19.0	1278	46	1278	46
CM93-20	170	20,041	2.5	2.15318	2.69	0.19931	1.55	0.58	1171.6	16.6	1166.1	18.7	1156	44	1156	44
CM93-21	77	9456	2.4	2.87946	3.16	0.24146	1.04	0.33	1394.3	13.1	1376.6	23.8	1349	58	1349	58
CM93-22	137	18,517	3.4	2.02490	3.86	0.18367	2.37	0.61	1087.0	23.7	1123.9	26.2	1196	60	1196	60
CM93-23	81	9792	2.4	2.05357	2.38	0.18669	1.30	0.55	1103.4	13.2	1133.5	16.2	1192	39	1192	39
CM93-24	290	24,554	1.4	2.59229	1.90	0.21719	1.00	0.53	1267.0	11.5	1298.5	13.9	1351	31	1351	31
CM93-25	166	26,332	2.9	3.12366	3.10	0.25076	1.11	0.36	1442.4	14.3	1438.5	23.8	1433	55	1433	55
CM93-26	411	10,252	1.4	1.62332	4.05	0.15169	3.51	0.87	910.4	29.8	979.3	25.4	1137	40	1137	40
CM93-27	138	17,229	1.6	2.15424	2.41	0.19744	1.07	0.44	1161.5	11.4	1166.4	16.7	1175	43	1175	43
CM93-28	170	21,901	1.9	2.46233	3.81	0.21320	2.62	0.69	1245.8	29.7	1261.0	27.6	1287	54	1287	54
CM93-29	154	13,549	2.3	2.10086	3.35	0.19564	2.47	0.74	1151.8	26.1	1149.1	23.1	1144	45	1144	45
CM93-30	91	4659	1.2	1.80077	4.38	0.16957	2.30	0.53	1009.7	21.5	1045.7	28.6	1122	74	1122	74
CM93-31	96	1732	2.6	2.13667	4.62	0.19167	2.77	0.60	1130.4	28.7	1160.7	32.0	1218	73	1218	73
CM93-32	94	22,136	1.9	1.77113	4.55	0.16915	1.13	0.25	1007.4	10.5	1034.9	29.5	1093	88	1093	88
CM93-33	19	9724	2.7	2.02631	4.62	0.17894										

Table 1 (continued)

Analysis	U (ppm)	206Pb 204Pb	U/Th	207Pb* 235U*	± (%)	206Pb 238U	± (%)	error corr.	206Pb 238U	± (Ma)	207Pb* 235U	± (Ma)	206Pb* 207Pb*	± (Ma)	Best age (Ma)	± (Ma)
CM93-43	399	34,491	3.3	2.92109	2.23	0.23149	1.78	0.80	1342.3	21.6	1387.4	16.9	1457	26	1457	26
CM93-44	239	12,350	2.7	1.41635	2.76	0.14434	1.32	0.48	869.2	10.7	895.8	16.4	962	49	962	49
CM93-45	396	35,274	9.3	2.26326	2.26	0.19704	1.22	0.54	1159.4	12.9	1200.9	15.9	1276	37	1276	37
CM93-46	267	16,899	5.1	0.68317	5.36	0.08429	1.06	0.20	521.7	5.3	528.7	22.1	559	115	522	5
CM93-47	59	8149	2.3	3.04317	3.19	0.24926	1.35	0.42	1434.7	17.4	1418.5	24.4	1394	55	1394	55
CM93-48	52	9100	1.3	2.92545	1.62	0.23549	1.00	0.62	1363.2	12.3	1388.5	12.3	1428	24	1428	24
CM93-49	123	12,955	2.4	1.72110	2.68	0.17198	1.44	0.54	1023.0	13.6	1016.4	17.2	1002	46	1002	46
CM93-50	227	23,072	1.4	3.14069	2.18	0.24240	1.58	0.72	1399.2	19.9	1442.7	16.8	1508	28	1508	28
CM93-51	208	13,714	2.4	1.69401	4.38	0.16614	2.12	0.48	990.8	19.5	1006.3	28.0	1040	77	1040	77
CM93-52	92	6413	2.6	1.53,234	6.72	0.15806	2.47	0.37	946.0	21.8	943.4	41.3	938	128	938	128
CM93-53	338	42,609	2.9	2.23292	2.42	0.20229	1.77	0.73	1187.6	19.2	1191.4	17.0	1198	33	1198	33
CM93-54	169	30,144	1.5	3.15542	3.95	0.24939	2.60	0.66	1435.3	33.5	1446.3	30.5	1463	57	1463	57
CM93-55	97	13,287	2.1	2.47940	2.43	0.20357	1.19	0.49	1194.5	13.0	1266.0	17.6	1390	41	1390	41
CM93-56	88	11,478	3.1	2.42515	4.54	0.21802	2.49	0.55	1271.4	28.7	1250.1	32.7	1214	75	1214	75
CM93-57	409	12,973	3.1	2.34693	2.70	0.19641	2.40	0.89	1156.0	25.4	1226.6	19.2	1353	24	1353	24
CM93-58	82	3763	0.8	1.53699	9.79	0.15207	7.92	0.81	912.5	67.4	945.3	60.3	1022	117	1022	117
CM93-59	108	18,918	2.0	3.98936	2.85	0.28682	1.07	0.37	1625.6	15.4	1632.0	23.2	1640	49	1640	49
CM93-60	79	10,338	0.8	2.17161	4.76	0.19476	1.00	0.21	1147.1	10.5	1172.0	33.1	1218	92	1218	92
CM93-61	148	15,664	1.1	2.12435	2.29	0.19818	1.35	0.59	1165.5	14.4	1156.8	15.8	1140	37	1140	37
CM93-62	282	20,536	2.4	2.86188	2.47	0.22970	1.96	0.79	1332.9	23.6	1371.9	18.6	1433	29	1433	29
CM93-63	85	10,012	1.6	2.19694	7.38	0.18755	6.20	0.84	1108.1	63.1	1180.1	51.6	1315	78	1315	78
CM93-64	50	7602	1.9	2.07461	2.84	0.18344	1.43	0.50	1085.7	14.3	1140.5	19.4	1246	48	1246	48
CM93-65	382	21,599	2.4	2.11015	2.16	0.18919	1.15	0.53	1117.0	11.8	1152.1	14.9	1219	36	1219	36
CM93-66	133	14,064	1.3	2.62546	2.89	0.22043	2.21	0.77	1284.2	25.7	1307.8	21.2	1347	36	1347	36

Central Cordillera of the Colombian Andes have yielded significant Grenvillian sources between 0.9 and 1.1 Ga (Fig. 1C, Ordoñez-Carmona, 2001; Cardona, 2003; Vinasco, 2004; Chew et al., 2007a,b, 2008; Cardona et al., 2008). These results clearly suggest that a Grenvillian belt was a major source region for these metasedimentary rocks.

7. Tectonic and paleogeographic correlations

Nd model ages of 1.6–1.9 Ga together with Pb isotope signatures from the Grenvillian inliers of the Colombian Andes suggest that the protoliths were formed on the margins of a continental block, probably the Amazonian Craton (Restrepo-Pace et al., 1997; Ordoñez-Carmona et al., 1999; Ordoñez-Carmona et al., 2006; Ruiz et al., 1999; Cordani et al., 2000, 2005). U-Pb detrital zircon ages from paragneisses which range between 1.3 Ga and 1.6 Ma and similar Nd model ages are correlatable with the temporal framework of the Rio Negro-Juruena and Rondonia – San Ignacio provinces of the Amazonian Craton (Cordani et al., 2000; Tassinari et al., 2000). Moreover the well defined 1.32–1.35 Ga zircon age population found in the Santa Marta, Santander and Guajira regions correlates with the Candeias or San Ignacio orogeny in the southwestern Amazonian Craton, which includes a widespread magmatic event of this age (Boger et al., 2005; Cordani et al., 2009; Santos et al., 2008). Therefore, the available zircon crystallization data from the Mesoproterozoic Colombian inliers (Fig. 1D) suggests they formed as sedimentary basins on the active margin of the Amazonian Craton. Metavolcanic and metaplutonic rocks in the Santa Marta and Garzón massifs would therefore represent subduction-related magmatism on this active margin. In the Garzón massif arc activity lasted until ca. 1160 Ma whereas in Santa Marta it is probably younger (Kroonenberg, 2001; Cordani et al., 2005; Cardona-Molina et al., 2006).

All Colombian Mesoproterozoic inliers record a common late metamorphic event between 0.9 and 1.0 Ga, although there is evidence of a more prolonged metamorphic evolution. Within the Garzón massif, the metamorphic event started by 1040 Ma whereas in the Guajira region there is evidence of a polymetamorphic record that initiated as early as 1160 Ma and lasted until ca. 993 Ma (Cordani et al., 2005).

The zircon data from the Eastern Peruvian Andes suggest that Mesoproterozoic crust constitutes a very important element of

the crustal basement on the Peruvian margin. The major peaks in the age distribution at 970 and 1060 Ma (Fig. 1B) are similar in age to two of the three Grenvillian granitoids sampled by Miškovic et al. (2009) and demonstrate the existence of the remnants of an orogenic and magmatic belt of Grenvillian age. Older peaks of 1210 Ma (Fig. 1C) would represent an older arc domain similar to that already discussed for Colombia (Cordani et al., 2005). The older Meso- and Paleoproterozoic zircon ages along with the Nd isotopic data from Paleozoic sedimentary and magmatic rocks of the Peruvian Andes show that the Amazonian Craton was the dominant source for the Paleozoic units and hence Grenvillian crust was likely a permanent feature along the margin (Chew et al., 2007a,b; Cardona et al., 2009).

Available geological data and indirect detrital constraints from the cratonic region of Colombia and Ecuador suggest that the Late Mesoproterozoic belt continues toward the craton margins (Pinson et al., 1962; Chew et al., 2007a,b). As previously mentioned, all Colombian terranes with the exception of the Garzón massif are likely to be remobilized. Recent paleomagnetic data from Jurassic volcano-sedimentary and Cretaceous sequences that overlie Grenvillian basement in Colombia show that these domains were displaced from southern latitudes similar to present day northern Peru and Ecuador (Fig. 4A, Bayona et al., 2006, submitted for publication). Most of the displacement probably occurred before the Early Cretaceous (Bayona et al., 2006, submitted for publication), probably triggered by oblique Jurassic subduction and later Pangea break-up that opened the proto-Caribbean Ocean in northern South America (Aspden et al., 1987; Pindell, 1993). The geochronological signature of the Grenvillian crustal basement in northern Peru supports a correlation with these Colombian terranes. Additional evidence for this comparison includes: (1) the Early Paleozoic magmatism and Silurian tectonism within these Grenvillian massifs. This was considered an indication of the allochthonous character of some of these Colombian units (Forero-Suarez, 1990; Toussaint, 1993; Restrepo-Pace, 1995; Ordoñez-Carmona et al., 2006), but it has been recently recognized within the Eastern Peruvian Andes (Chew et al., 2007a,b; Cardona et al., 2009; Miškovic et al., 2009); (2) Ordovician graptolites in the sedimentary cover have affinities with graptolites reported in northern Argentina (Velez and Villarroel, 1993; Moreno et al., 2008); (3) a similar upper Triassic–Lower Jurassic ammonite association is present in northern Peru and the San Lucas Serranía at the northern end of the Central Cordillera of Colombia (Geyer, 1969).

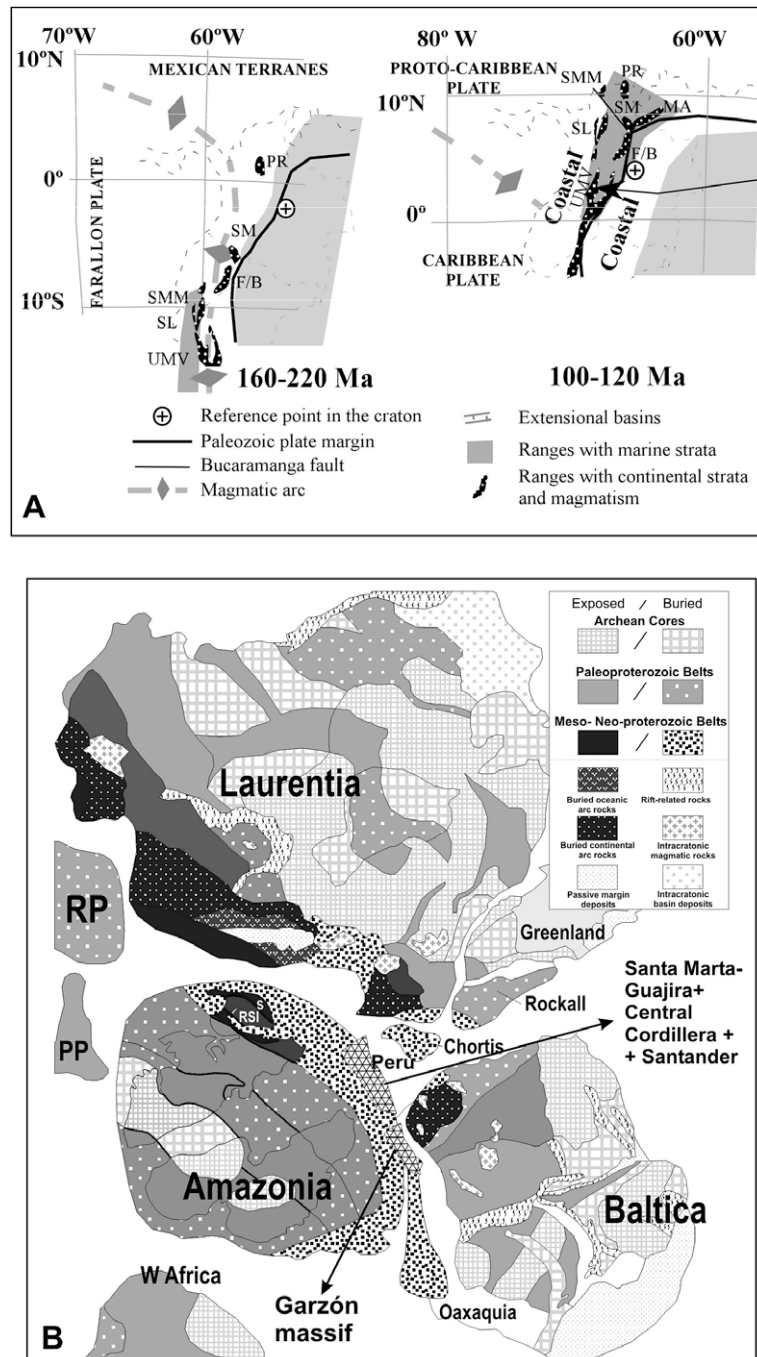


Fig. 4. (A) Mesozoic paleogeographic reconstructions of Jurassic segments with Grenvillian crustal basement (after Bayona et al., 2006, 2009). F/B: Floresta massif/ Bucaramanga area; MA: Merida Andes; PR: Perija Range; SL: San Lucas range; SM: Santander massif; SMM: Santa Marta massif; UMV: Upper Magdalena Valley. (B) Rodinia reconstruction including Grenvillian crustal domains of the northern Andes and Mexico (after Li et al., 2008).

Late Paleozoic tectonic reconstructions of Pangea show a major spatial overlap between northern South America and the Paleozoic and Proterozoic terranes that formed the core of central and southern Mexico and Middle America (Rowley and Pindell, 1989; Dickinson and Lawlor, 2001). This new paleogeographic scenario (Bayona et al., 2006, submitted for publication) for the Jurassic partly resolves this problem with some of the Colombian terranes (such as Santa Marta, Santander and the Central Cordillera) located in northern Peru – Ecuador with the Mexican terranes situated on the Colombian margin.

Geological, geochronological and isotopic data suggest that the Grenvillian rocks in Mexico are allochthonous to North America

and formed in proximity to the margin of the Amazonian Craton, with possible counterparts in some of the Colombian inliers such as Garzón and Santa Marta (Ortega-Gutiérrez et al., 1995; Restrepo-Pace et al., 1997; Keppie and Ortega-Gutiérrez, 1999; Ruiz et al., 1999; Keppie et al., 2003; Gillis et al., 2005; Keppie and Dostal, 2007).

These Grenvillian Mexican rocks are included within the composite Oaxaquia terrane (or microcontinent) characterized by the formation of a juvenile Mesoproterozoic arc and extensional plutonism between 1230 and 1115 Ma, followed by the intrusion of anorthosite suites at ca. 1010 Ma and a widespread major granulite-facies metamorphic event between 990 and 975 Ma (Ruiz

et al., 1988, 1999; Yañez, et al., 1991; Ortega-Gutierrez et al., 1995; Keppie and Ortega-Gutierrez, 1999; Lawlor et al., 1999; Weber and Köhler, 1999; Lopez et al., 2001; Solari et al., 2003; Keppie et al., 2003; Keppie and Dostal, 2007). Additionally, there is evidence for an older ca. 1100 Ma deformational event. The correlation, tectonic and temporal framework of the Grenvillian units of the Northern Andes and Oaxaquia also place them on the margins of the Amazonian Craton, where they form part of the arcs related to the closure of Mesoproterozoic oceans and the juxtaposition of the continental masses within the Rodinia Supercontinent (Hoffman, 1991; Restrepo-Pace et al., 1997; Cordani et al., 2005; Keppie et al., 2001, 2003; Ordóñez-Carmona et al., 2006; Li et al., 2008).

8. Rodinian paleogeographic implications

It has been long postulated that the Late Mesoproterozoic Grenville Province in North America was formed by individual collisions involving three separate crustal blocks: the cratons of Kalahari, Amazonia, and Baltica (Hoffman, 1991).

The Grenville orogeny of Laurentia has been subdivided into several phases which record ongoing Late Mesoproterozoic ocean closure (Rivers 1997; Wasteneys et al., 1999; Gower and Krogh, 2002; Tollo et al., 2004). The older events (the 1220–1240 Ma Elsevierian and 1190–1140 Ma Shawingian phases) are mostly related to arc and terrane collisions in the southwest Grenville Province (Rivers, 2008). The other two main phases are related to continental collisional events that include the diachronous and widespread Ottawa event (1080–1020 Ma) and a younger Rigolet event at 1000–980 Ma. Recent models have considered this two phase orogenic model as reflecting a prolonged continental collision with an intervening stage of orogenic collapse followed by foreland propagation of the deformation front (Rivers, 2008).

The tectonic record of the temporally equivalent Sunsas orogen in the southwest Amazonian Craton in Brazil and Bolivia has been the subject of several recent reviews (e.g., Tohver et al., 2004, 2005, 2006; Boger et al., 2005; Cordani and Teixeira, 2007a,b; Santos et al., 2008). The Sunsas Orogen includes evidence of an early 1.2–1.15 Ga remobilization of older basement along shear zones, 1.1–1.08 Ga amphibolite to granulite-facies metamorphism, several post-tectonic and anorogenic phases of magmatism between 1.1 and 0.97 Ga, with final cooling of the orogen constrained at 0.9–1.0 Ga. Paleomagnetic and isotopic constraints suggest that the entire Grenvillian orogeny on the Amazonian Craton took place in a single transpressive with Laurentia and probably some intervening microcontinents beginning at ca. 1.2 Ga (Tohver et al., 2002, 2004, 2006; D'Agrella-Filho et al., 2008). However alternative models show that the nature of the colliding continent is far from being resolved (Cordani and Teixeira, 2007a,b; Li et al., 2008; Santos et al., 2008; Chew et al., 2008).

The extensive 1.0–0.9 Ga high-grade metamorphic event present in the Colombian and Mexican inliers, the possible continuity of magmatism from 1160 to 1080 Ma in some of these inliers, along with the sporadic Grenvillian granitoids and detrital zircon populations from the Peruvian margin north of 10° south, suggest that they represent an orogenic segment different to the Sunsas type belt exposed in the southwest Amazonian Craton.

Whether Laurentia or another large crustal block represents the colliding entity with the SW Amazonian Craton, the geometry and dimension of the western margin of the Amazonian Craton in the proto-Andean margin suggests that more than one continental mass must have interacted during the Grenvillian event and create different orogenic segments.

We therefore agree with recent continental reconstruction models in which the northwestern margin of the Amazonian Craton was interacting with Baltica and other continental masses such

as Oaxaquia (Fig. 4B, Keppie and Dostal, 2007; Li et al., 2008), whereas Sunsas (southwestern Amazonia) was interacting with Laurentia. Within this configuration, the Grenvillian units of the northern Andes of Colombia, Ecuador and northern Peru together with Oaxaquia form the core of a laterally composite orogen. The identification of terrane or crustal transfer during the Grenvillian collisional phases is a major step in refining these reconstructions. Although more data still needs to be acquired from the Grenvillian inliers of the Andes and the Amazonian Craton, there is some evidence that suggest that this transfer took place during collision: (1) Pb isotopical variations and similarities within and between Oaxaquia and the Colombian massifs (Ruiz et al., 1999). (2) Lateral variations in the tectonic setting from arc to extensional magmatic systems both in Oaxaquia and between the Santa Marta volcanics and Garzón plutonic rocks (Cordani et al., 2005; Cardona-Molina et al., 2006; Keppie and Dostal, 2007), and (3) the existence of an arc system and extensional magmatism between 1160 and 1035 Ma in the Sveconorwegian Province of SW Norway (Bingen and Breemen, 1998; Bogdanova et al., 2008) which overlaps with the magmatic record of the Colombian massifs and Oaxaquia, as well as the major zircon crystallization ages from Peru (Weber and Hecht, 2003; Keppie et al., 2001, 2003).

9. Conclusions

Geological and geochronological data from the Grenvillian inliers and detrital signatures on younger Paleozoic orogens from the Northern Andes, suggest that that this region along with correlative terranes exposed Middle America and Mexico, represent a separate composite Grenvillian orogen. These fragments differ from the Sunsas province in the Amazon Craton and the North American Grenville province, and were formed on the northwest margin of the Amazonian Craton by microcontinent accretion and interaction with the Sveconorwegian province on Baltica.

Acknowledgments

We gratefully thank the editors for their invitation to contribute to this volume. ECOPETROL-ICP, INVEMAR and INGEOMINAS are acknowledged for allowing access to the sample collected in the Santa Marta Massif. Comments and reviews from two anonymous reviewers. We acknowledge partial support for analytical work received from the Fundación para el Apoyo de la Investigación y la Cultura del Banco de la República de Colombia, project 2289 and the São Paulo State Research Agency (FAPESP), Grant 02/072488-3. A. C. acknowledge U. Cordani for his continuous academic support.

Appendix 1. Analytical techniques

U-Pb data presented in this study were undertaken by laser ablation multicollector inductively coupled plasma mass spectrometry (LA-MC-ICP-MS) at the Arizona LASERCHRON laboratory following the procedures described by Gehrels et al. (2008). Unknowns and standard zircons were mounted in the central portion of the epoxy mount to reduce possible fractionation effects. The zircon grains analyzed were selected randomly from the population on the sample mount. For detrital samples the core of grains were analyzed to avoid possible thin metamorphic overgrowths. Zircon crystals were analyzed with a VG Isoprobe multicollector ICPMS equipped with nine Faraday collectors, an axial Daly collector, and four ion-counting channels. The Isoprobe is equipped with an ArF Excimer laser ablation system, which has an emission wavelength of 193 nm. The collector configuration allows measurement of ^{204}Pb in the ion-counting channel while ^{206}Pb , ^{207}Pb , ^{208}Pb , ^{232}Th

and ^{238}U are simultaneously measured with Faraday detectors. All analyses were conducted in static mode with a laser beam diameter of 35–50 μm , operated with an output energy of $\sim 32 \text{ mJ}$ (at 23 kV) and a pulse rate of 9 Hz. Each analysis consisted of one 20-s integration on peaks with no laser firing and 20 1-s integrations on peaks with the laser firing. ^{204}Hg contribution to the ^{204}Pb mass position was removed by subtracting on-peak background values. Inter-element fractionation was monitored by analyzing an in-house zircon standard, which has a concordant TIMS age of $564 \pm 4 \text{ Ma}$ (2σ) (Gehrels, unpublished data). This standard was analyzed once for every five unknowns in detrital grains. U and Th concentrations were monitored by analyzing a standard (NIST 610 Glass) with $\sim 500 \text{ ppm}$ Th and U. The Pb isotopic ratios were corrected for common Pb, using the measured ^{204}Pb , assuming an initial Pb composition according to Stacey and Kramers (1975).

The uncertainties on the age of standard, the calibration correction from standard, the composition of the common Pb, and the decay constant uncertainty are grouped together and are known as the systematic error. For the zircon analyses in this study the systematic errors range between $\sim 1.0\%$ and 1.4% for the $^{206}\text{Pb}/^{238}\text{U}$ ratio and $\sim 0.8\%$ and 1.1% for the $^{207}\text{Pb}/^{206}\text{Pb}$ ratio. Analytical results are presented in Table 1.

References

- Ashwal, L.D., 1993. Anorthosites. Springer-Verlag, Berlin. 422p.
- Aspden, J.A., McCourt, W.J., Brook, M., 1987. Geometrical control of subduction related magmatism: the Mesozoic and Cenozoic plutonic history of western Colombia. *Journal of the Geological Society, London* 144, 893–905.
- Banks, P., 1975. Basement rocks bordering the Gulf of México and the Caribbean Sea. In: Nairn, A.E., Stehlí, F.G. (Eds.), *The Ocean Basins and Margins*, vol. 3. The Gulf of Mexico and the Caribbean, p. 191.
- Bayona, G., Rapalini, V., Constanzo-Alvarez, V., 2006. Paleomagnetism in Mesozoic rocks of the northern Andes and its implications in Mesozoic tectonics of northwestern South America. *Earth, Planets and Space* 58, 1255–1272.
- Bayona, G., Jiménez, G., Silva, C., Cardona, A., Montes, C., Roncancio, J., submitted for publication. Paleomagnetic data uncovered from Mesozoic units of the Santa Marta Massif: constrain for paleogeographic and paleotectonic evolution of the NW corner of the South America plate. *Journal of South American Earth Sciences*.
- Bayona, G., Jiménez, G., Silva, C., Cardona, A., Montes, C., Roncancio, J., Cordani, U., 2009. Paleomagnetic data and K-Ar ages from Mesozoic units of the Santa Marta Massif: A preliminary interpretation for block rotation and translations. *Journal of South American Earth Sciences*, in press. Available from: <
- Bingen, B., Breemen, Van, 1998. Tectonic regimes and terrane boundaries in the high-grade Sveconorwegian belt of SW Norway, inferred from U-Pb zircon geochronology and geochemical signature of augen gneiss suites. *Journal of the Geological Society* 155, 143–154.
- Bogdanova, S.V., Bingen, B., Gorbatschev, R., Kheraskova, T.N., Kozlov, V.I., Puchkov, V.N., Volozh, Yu.A., 2008. The East European Craton (Baltica) before and during the assembly of Rodinia. *Precambrian Research* 160, 23–45.
- Boger, S.D., Raetz, M., Giles, D., 2005. U-Pb age data from the Sunas region of eastern Bolivia, evidence for the allochthonous origin of the Paragua block. *Precambrian Research* 139, 121–146.
- Burkley, L.A., 1976. Geochronology of the Central Venezuelan Andes. PhD Thesis, Case Western Reserve University, 150p.
- Cardona, A., 2003. Correlações entre fragmentos do embasamento pre-Mesozoico da terminação setentrional dos Andes Colombianos, com base em dados isotópicos e geocronológicos. Dissertação de Mestrado, Universidade de São Paulo, Brazil. 119p.
- Cardona, A., Cordani, U., Sanchez, A., 2007. Metamorphic, geochronological and constraints from the pre-Peruvian basement of the eastern Peruvian (10°S): a Paleozoic extensional-accretionary orogen? 20th Colloquium on Latin American Earth Sciences, April 11–13, Kiel, Germany. Abstracts volume, pp. 29–30.
- Cardona, A., Cordani, U., Nutman, A., 2008. U-Pb SHRIMP zircon, $^{40}\text{Ar}/^{39}\text{Ar}$ geochronology and Nd isotopes from gneissic and granitoid rocks of the Illescas massif, Perú: a southern extension of a fragmented Late Paleozoic orogen? VI South American Symposium on Isotope Geology San Carlos de Bariloche – Argentina. Extended Abstracts.
- Cardona, A., Cordani, U.G., Ruiz, J., Valencia, V.A., Armstrong, R., Nutman, A., Sanchez, A., 2009. U/Pb zircon and Nd isotopic signatures of the pre-Mesozoic metamorphic basement of the Eastern Peruvian Andes: growth and Provenance of a Late Neoproterozoic to Carboniferous accretionary orogen on the Northwest margin of Gondwana. *Journal of Geology* 117, 285–305.
- Cardona-Molina, A., Cordani, U.G., Macdonald, W., 2006. Tectonic correlations of pre-Mesozoic crust from the northern termination of the Colombian Andes, Caribbean region. *Journal of South American Earth Sciences* 21, 337–354.
- Cawood, P.A., 2005. Terra Australis orogen: Rodinia breakup and development of the Pacific and Iapetus margins of Gondwana during the Neoproterozoic and Paleozoic. *Earth-Science Reviews* 69, 249–279.
- Cawood, P.A., McCauley, P.J.A., Dunning, G.R., 2001. Opening Iapetus: constraints from the Laurentian margin in Newfoundland. *Geological Society of America Bulletin* 113, 443–453.
- Cediel, F., Shaw, R., Cáceres, C., 2003. Tectonic assembly of the Northern Andean block. In: Bartolini, C., Buffler, R., Blickwede, J. (Eds.), *The Circum-Gulf of Mexico and the Caribbean: Hydrocarbon Habitats, Basin Formation and Plate Tectonics*, vol. 79. American Association of Petroleum Geologists, Memoir, pp. 815–848.
- Chew, D.M., Schaltegger, U., Košler, J., Whitehouse, M.J., Gutjahr, M., Spikings, R.A., Mišković, A., 2007a. U-Pb geochronologic evidence for the evolution of the Gondwanan margin of the north-central Andes. *Geological Society of America Bulletin* 119, 697–711.
- Chew, D.M., Kirkland, C.L., Schaltegger, U., Goodhue, R., 2007b. Neoproterozoic glaciation in the Proto-Andes: tectonic implications and global correlation. *Geology* 35, 1095–1099.
- Chew, D.M., Magna, T., Kirkland, C.L., Mišković, A., Cardona, A., Spikings, A., Schaltegger, U., 2008. Detrital zircon fingerprint of the Proto-Andes: evidence for a Neoproterozoic active margin? *Precambrian Research* 167, 186–200.
- Cordani, U.G., Teixeira, W., 2007a. Proterozoic accretionary belts in the Amazonian Craton. In: Hatcher Jr., R.D., Carlson, M.P., McBride, J.H., Martínez-Catalán, J.R. (Eds.), *4-D Framework of Continental Crust*, vol. 200. Geological Society of America, Memoir, pp. 297–320.
- Cordani, U.G., Teixeira, W., 2007b. Proterozoic accretionary belts in the Amazonian Craton. In: Hatcher Jr., R.D., Carlson, M.P., McBride, J.H., Martínez-Catalán, J.R. (Eds.), *4-D Framework of Continental Crust*, vol. 200. Geological Society of America, Memoir, pp. 297–320.
- Cordani, U.G., Sato, K., Teixeira, W., Tassinari, C.C.G., Basei, M.A.S., 2000. Crustal evolution of the South American Platform. In: Cordani, U.G., Milani, E.J., Thomaz, A., Campos, D.A. (Eds.), *Tectonic Evolution of South America*. Rio de Janeiro: 31st International Geological Congress, pp. 19–40.
- Cordani, U.G., Cardona, A., Jimenez, D., Liu, D., Nutman, A.P., 2005. Geochronology of Proterozoic basement inliers from the Colombian Andes: tectonic history of remnants from a fragmented Grenville belt. In: Vaughan, A.P.M., Leat, P.T., Pankhurst, R.J. (Eds.), *Terrane Processes at the Margins of Gondwana*. Geological Society of London, Special Publication 246, pp. 329–346.
- Cordani, U.G., Teixeira, W., D'Agrella-Filho, M.S., Trindade, R.I., 2009. The position of the Amazon Craton in Supercontinents. *Gondwana Research* 115, 396–407.
- D'Agrella-Filho, M.S., Tohver, E., Santos, J.O.S., Elming, S.-A., Trindade, R.I.F., Pacca, I.I.G., Geraldus, M.C., 2008. Direct dating of paleomagnetic results from Precambrian sediments in the Amazon Craton: evidence for Grenvillian emplacement of exotic crust in SE Appalachians of North America. *Earth and Planetary Science Letters* 267, 188–199.
- Dalmayrac, B., Laubacher, B., Marocco, R., 1988. Caracteres generales de la evolución geológica de los Andes Peruanos, vol. 12. Instituto Geológico Minero y Metalúrgico, Boletín, 313p.
- Dickinson, W.R., Lawlor, T.F., 2001. Carboniferous to Cretaceous assembly and fragmentation of Mexico. *Geological Society of America Bulletin* 113, 1142–1160.
- Fee-Codecido, G., Smith, F., Aboud, N., Di Giacomo, E., 1984. Basement Paleozoic rocks of the Venezuelan Llanos Basin, vol. 162. Geological Society of America, Memoir, pp. 175–187.
- Forero-Suarez, A., 1990. The basement of the Eastern Cordillera, Colombia: an allochthonous terrane in northwestern South America. *Journal of South American Earth Sciences* 3, 141–151.
- Gehrels, G., Valencia, V., and Ruiz, J., 2008. Enhanced precision, accuracy, efficiency, and spatial resolution of U-Pb ages by laser ablation-multicollector-inductively coupled plasma-mass spectrometry. *Geochemistry, Geophysics, Geosystems*, doi:10.1029/2007GC001805.
- Geyer, O., 1969. La fauna de ammonitas del perfil típico de la Formación Morrocoy. *Primer Congreso Colombiano de Geología, Memorias*, Bogotá, pp. 111–134.
- Gillis, R.J., Gehrels, G.E., Ruiz, J., Flores De Dios, L., 2005. Detrital zircon provenance of Cambrian-Ordovician and Carboniferous strata of the Oaxaca terrane, southern Mexico. *Sedimentary Geology* 182, 87–100.
- Goldstein, S.L., Arndt, N.Y., Stallard, R.E., 1997. The history of a continent from U-Pb ages of zircons from Orinoco River sand and Sm-Nd isotopes in Orinoco river sediments. *Chemical Geology* 139, 269–284.
- Gower, C.F., Krogh, T.E., 2002. A U-Pb geochronological review of the Proterozoic history of the eastern Grenville Province. *Canadian Journal of Earth Sciences* 39, 795–829.
- Grande, S., Urbani, F., Mendi, D., 2007. Presencia de un basamento grenvilliano de alto grado en Venezuela noroccidental. Estudio en progreso. IX Congreso Geoógico Venezolano, Caracas, Venezuela, +16p., en CD.
- Hoffman, P.A., 1991. Did the breakout of Laurentia turn Gondwanaland inside-out? *Science* 252, 1409–1411.
- Jiménez-Mejía, D.M., Juliani, C., Cordani, U.G., 2006. P-T-t conditions of high-grade metamorphic rocks of the Garzón Massif, Andean basement, SE Colombia. *Journal of South American Earth Sciences* 21, 322–336.
- Johnson, M.J., 1991. Controls on the composition of fluvial sands from tropical weathering environment sands of the Orinoco River drainage basin, Venezuela and Colombia. *Geological Society of America Bulletin* 103, 1622–1647.

- Kay, S.M., Orrell, S., Abbruzzi, J.M., 1996. Zircon and whole rock Nd–Pb isotopic evidence for a Grenville age and a Laurentian origin for the basement of the PreCORDILLERA in Argentina. *Journal of Geology* 104, 637–648.
- Keppie, J.D., Ortega-Gutiérrez, F., 1999. Middle American Precambrian basement: a missing piece of the reconstructed 1-Ga orogen. In: Ramos, V.A., Keppie, J.D. (Eds.), *Laurentia and Gondwana Connections before Pangea*. Geological Society of America Special Paper 336, pp. 183–198.
- Keppie, J.D., Ramos, V., 1999. Odyssey of terranes in the Iapetus and Rheic oceans during the Paleozoic. In: Ramos, V.A., Keppie, J.D. (Eds.), *Laurentia and Gondwana Connections before Pangea*. Geological Society of America Special Paper 336, pp. 267–276.
- Keppie, J.D., Dostal, J., Ortega-Gutiérrez, F., Lopez, R., 2001. A Grenvillian arc on the margin of Amazonia: evidence from the southern Oaxacan Complex, southern Mexico. *Precambrian Research* 112, 165–181.
- Keppie, J.D., Dostal, J., Cameron, K.L., Solari, L.A., Ortega-Gutiérrez, F., Lopez, R., 2003. Geochronology and geochemistry of Grenvillian igneous suites in the northern Oaxacan complex, southern Mexico: tectonic implications. *Precambrian Research* 120, 365–389.
- Keppie, J.D., Dostal, J., 2007. Rift-related basalts in the 1.2–1.3 Ga granulites of the northern Oaxacan Complex, southern Mexico: evidence for a rifted arc on the northwestern margin of Amazonia. *Proceedings of the Geologist Association* 118, 63–74.
- Kroonenberg, G.S., 1982. A Grenvillian granulite belt in the Colombian Andes and its relations to the Guiana Shield. *Geologie en Mijnbouw* 61, 325–333.
- Kroonenberg, S.B., 2001. La colisión continental entre Amazonia y Laurentia 1100 Ma atrás. *Coloquio sobre el Precámbrico de Colombia*, Bogotá, Resumenes, Ingeominas, pp. 12–15.
- Lawlor, P.J., Ortega-Gutiérrez, F., Cameron, K.L., Ochoa-Caramillo, H., Lopez, R., Sampson, D.E., 1999. U–Pb geochronology, geochemistry and provenance of the Grenvillian Huiznopalna Gneiss of Eastern Mexico. *Precambrian Research* 94, 73–99.
- Li, Z.X., Bogdanova, S.V., Collins, A.S., Davidson, A., De Waele, B., Ernst, R.E., Fitzsimons, I.C.W., Fuck, R.A., Gladkochob, D.P., Jacobs, J., Karlstrom, K.E., Lu, S., Natopov, L.M., Pease, V., Pisarevsky, S.A., Thrane, K., Vernikovsky, V., 2008. Assembly, configuration and breakup of Rodinia: a synthesis. *Precambrian Research* 160, 179–210.
- Litherland, M., Aspden, J.A., Jemielita, R.A., 1994. The Metamorphic Belts of Ecuador, vol. 11. Overseas Memoir of the British Geological Survey, 147p.
- Loewy, S.L., Connelly, J.N., Dalziel, I.W.D., 2004. An orphaned basement block: the Arequipa-Antofalla basement of the central Andean margin of South America. *Geological Society of America Bulletin* 116, 171–187.
- Lopez, R., Cameron, K.L., Jones, N.W., 2001. Evidence for Paleoproterozoic, Grenvillian, and Pan-African age Gondwanan crust beneath northeastern Mexico. *Precambrian Research* 107, 195–214.
- MacDonald, W.D., Hurley, P.M., 1969. Precambrian gneisses from northern Colombia, South America. *Geological Society of America Bulletin* 80, 1867–1872.
- Mišković, A., Schaltegger, U., Spikings, R.A., Chew, D.M., Košler, J., 2009. Tectonomagmatic evolution of Western Amazonia: geochemical characterization and zircon U–Pb geochronologic constraints from the Peruvian Eastern Cordillera granitoids. *Geological Society of America Bulletin*, in press.
- Moreno, M., Gómez, A., Castillo, H., 2008. Graptolitos del Ordovícico y Geología de los Afloramientos del Río Venado (Norte del Departamento del Huila), vol. 30. Universidad Industrial de Santander, Bucaramanga, Boletín de Geología, pp. 9–19.
- Nance, R.D., Linnemann, U., 2008. The Rheic ocean: origin, evolution, and significance. *GSA Today* 18, 4–12.
- Noble, S.R., Aspden, J.A., Jemielita, R., 1997. Northern Andean crustal evolution: new U–Pb geochronological constraints from Ecuador. *Geological Society of America Bulletin* 109, 789–798.
- Ordoñez-Carmona, O., 2001. Caracterizacão isotópica Rb–Sr e Sm–Nd dos principais eventos magnéticos nos Andes Colombianos. Tesse de Doutorado, Universidade de Brasília, Brasília, Brazil. 176p.
- Ordoñez-Carmona, O., Pimentel, M.M., De Moraes, R., Restrepo, J.J., 1999. Rocas Grenvillianas en la región de Puerto Berrio – Antioquia, vol. 23. Revista de la Academia Colombiana de Ciencias Exactas, Físicas y Naturales, pp. 225–232.
- Ordoñez-Carmona, O., Pimentel, M.M., and De Moraes, R., 2002. Granulitas de Los Mangos: un fragmento grenviliense en la parte SE de la Sierra Nevada de Santa Marta, vol. 26. Revista de la Academia Colombiana de Ciencias Exactas, Físicas y Naturales, pp. 169–179.
- Ordoñez-Carmona, O., Restrepo, J.J., Pimentel, M.M., 2006. Geochronological and isotopical review of pre-Devonian crustal basement of the Colombian Andes. *Journal of South American Earth Sciences* 21, 372–382.
- Ordoñez-Carmona, O., Restrepo, J.J., Cuadros, F., Minota, J.A., Londoño, C., Alvares, M.J., 2007. Rocas metamórficas de alto grado en la Serranía de San Lucas. *Boletín de Ciencias de la Tierra* 22, 131–132.
- Ortega-Gutiérrez, F., Ruiz, F., Centeno-García, E., 1995. Oaxaquia, a Proterozoic microcontinent accreted to North America during the Late Paleozoic. *Geology* 23, 1127–1130.
- Pindell, J.L., 1993. Evolution of the Gulf of Mexico and the Caribbean. In: Donovan, S.K., Jackson, T.A. (Eds.), *University of the West Indies Publisher's Association. Caribbean Geology: An Introduction*, pp. 13–39.
- Pinson, W.H., Hurley, P.M., Mencher, E., Fairbairn, H.W., 1962. K–Ar and Rb–Sr ages of biotites from Colombia, South America. *Geological Society of America Bulletin* 73, 907–910.
- Pratt, W.T., Duque, P., Ponce, M., 2005. An autochthonous geological model for the eastern Andes of Ecuador. *Tectonophysics* 399, 251–278.
- Priem, H.N.A., Andriessen, P., Boelrijk, N.A.I.M., De Boorder, H., Hebeda, E.H., Huguet, A., Verduren, E., Verschure, R., 1982. Geochronology of the Precambrian in the Amazonas region of southeastern Colombia (Western Guiana Shield). *Geologie en Mijnbouw* 61, 229–242.
- Priem, H.N.A., Beets, D.J., Th, E.A., 1986. Precambrian rocks in an Early Tertiary conglomerate in Bonaire, Netherlands Antilles (southern Caribbean Borderland): evidence for a 300 Km eastward displacement relative to the South American mainland? *Geologie en Mijnbouw* 65, 35–40.
- Priem, H.N.A., Kroonenberg, S.B., Boelrijk, N.A.I.M., Hebeda, E.H., 1989. Rb–Sr and K–Ar evidence for the presence of a 1.6 Ga basement underlying the 1.2 Ga Garzón-Santa Marta Granulite Belt in the Colombian Andes. *Precambrian Research* 42, 315–324.
- Ramos, V.A., 2008. The basement of the Central Andes: the Arequipa and related terranes. *Annual Review of Earth and Planetary Sciences* 36, 289–324.
- Ramos, V.A., Basei, M.A., 1997. Gondwanan, Perigondwanan, and exotic terranes of southern South America. 1st South American Symposium of Isotope Geology. São Paulo, Brazil, pp. 250–252.
- Restrepo-Pace, P., 1995. Late Precambrian to Early Mesozoic tectonic evolution of the Colombian Andes, based on new Geochronological, Geochemical and isotopic data. University of Arizona PhD Thesis, Unpublished, 195p.
- Restrepo-Pace, P.A., Ruiz, J., Gehlers, G., Cosca, M., 1997. Geochronology and Nd isotopic data of Grenville-age rocks in the Colombian Andes: new constraints for Late Proterozoic-Early Paleozoic paleocontinental reconstructions of the Americas. *Earth and Planetary Science Letters* 150, 427–441.
- Rivers, T., 1997. Lithotectonic elements of the Grenville Province. review and tectonic implications. *Precambrian Research* 86, 117–154.
- Rivers, T., 2008. Assembly and preservation of lower, mid, and upper orogenic crust in the Grenville Province—implications for the evolution of large hot long-duration orogens. *Precambrian Research* 167, 237–259.
- Rowley, D.B., Pindell, J.L., 1989. End Paleozoic-Early Mesozoic western Pangean reconstruction and its implications for the distribution of Precambrian and Paleozoic rocks around Meso-America. *Precambrian Research* 42, 411–444.
- Rubatto, D., 2002. Zircon trace element geochemistry: distribution coefficients and the link between U–Pb ages and metamorphism. *Chemical Geology* 184, 123–138.
- Ruiz, J., Patchett, J., Ortega-Gutiérrez, F., 1988. Proterozoic and Phanerozoic Basement terranes of Mexico from Nd isotopic studies. *Geological Society of America Bulletin* 100, 274–281.
- Ruiz, J., Tosdal, R.M., Restrepo, P. A., and Murillo-Muñeton, G., 1999. Pb Isotope evidence for Colombian-southern Mexico connections in the Proterozoic. In: Ramos, V.A., Keppie, J.D. (Eds.), *Laurentia and Gondwana Connections before Pangea*. GSA Special Paper 336, pp. 183–198.
- Santos, J.O.S., Rizzotto, G.J., Potter, P.E., McNaughton, N.J., Matos, R.S., Hartmann, L.A., Chemale, F., Quadros, M.E.S., 2008. Age and autochthonous evolution of the Sunsás orogen in West Amazon Craton based on mapping and U–Pb geochronology. *Precambrian Research* 165, 120–152.
- Solari, L.A., Keppie, J.D., Ortega-Gutiérrez, E., Cameron, H.L., Lopez, R., Haines, E., 2003. 990 Ma and 1100 Ma Grenvillian tectonothermal events in the northern Oaxacan Complex, Southern Mexico: roots of an orogen. *Tectonophysics* 356, 257–282.
- Stacey, J.S., Kramers, J.D., 1975. Approximation of the terrestrial lead isotope evolution by a two-stage model. *Earth and Planetary Science Letters* 26, 207–221.
- Tassinari, C.G., Bettencourt, J.S., Geraldes, M.C., Macambira, M., Lafon, J.M., 2000. The Amazonian Craton. In: Cordani, U.G., Milani, E.J., Thomaz, A., Campos, D.A. (Eds.), *Tectonic evolution of South America. Rio de Janeiro: 31st International Geological Congress*, pp. 41–96.
- Thornburg, T., Kulm, L.D., 1981. Sedimentary basins of the Peru continental margin: structure, stratigraphy, and Cenozoic tectonics from 6°S to 16°S latitude. *Geological Society of America Memoir* 154, 393–422.
- Tohver, E., van der Pluijm, B.A., Van der Voo, R., Rizzotto, G., and Scandolara, J.E., 2002. Paleogeography of the Amazon craton at 1.2 Ga: Early Grenvillian collision with the Llano segment of Laurentia. *Earth and Planetary Science Letters*, 199, 185–200.
- Tohver, E., van der Pluijm, B.A., Mezger, K., Scandolara, J.E., and Essene, E.J., 2004. Significance of the Nova Brasilândia Metasedimentary Belt in western Brazil: redefining the Mesoproterozoic boundary of the Amazon craton. *Tectonics*, 23, TC6004. doi:10.1029/2003TC001563.
- Tohver, E., van der Pluijm, B.A., Scandolara, J.E., Essene, E.J., 2005. Late Mesoproterozoic deformation of SW Amazonia (Rondonia, Brazil): geochronological and structural evidence for collision with Southern Laurentia. *Journal of Geology* 113, 309–323.
- Tohver, E., Teixeira, W., van der Pluijm, B.A., Geraldes, M.C., Bettencourt, J.S., Rizzotto, G., 2006. Restored transect across the exhumed Grenville orogen of Laurentia and Amazonia, with implications for crustal architecture. *Geology* 34, 669–672.
- Tollo, R.P., Corriveau, L., McLellan, J., Bartholemew, M.J., 2004. Proterozoic evolution of the Grenville orogen in North America: an introduction. In: Tollo, R.P., Corriveau, L., McLellan, J., Bartholemew, M.J. (Eds.), *Proterozoic Tectonic Evolution of the Grenville Orogen in North America*, vol. 197. Geological Society of America, Memoir, Boulder, CO, pp. 1–18.
- Toussaint, J.F., 1993. Evolución geológica de Colombia. Precámbrico–Paleozóico. Universidad Nacional de Colombia, Medellín. 129p.

- Tschanz, C., Richard, F.M., Cruz, B.J., Harald, H.M., Gerald, T.C., 1974. Geologic evolution of the Sierra Nevada de Santa Marta, Northeastern Colombia. Geological Society American Bulletin 85, 273–284.
- Velez, M.I., Villarroel, C. 1993. La fauna de trilobites de la Formación el Higado (Ordovícico Medio), aflorante en la Serranía de las Minas (Huila-Colombia), vol. 2. VI Congreso Colombiano de Geología, Medellín, Colombia, Memorias, pp. 169–180.
- Vesga, C.J., Barrero, D., 1978. Edades K/Ar en rocas ígneas y metamórficas de la Cordillera Central de Colombia y su implicación geológica. In: II Congreso Colombiano de Geología, Bogotá, Resumenes.
- Vinasco, C.J., 2004. Evolução crustal e história dos granitóides Permo-Triássicos dos Andes do Norte. Tese de Doutorado, Universidade de São Paulo. 120p.
- Vinasco, C.J., Cordani, U.G., González, Weber, M., Pelaez, C., 2006. Geochronological, isotopic, and geochemical data from Permo-Triassic granitic gneisses and granitoids of the Colombian Central Andes. Journal of South American Earth Sciences 21, 355–371.
- Ward, E.D., Goldsmith, R., Cruz, B.J., Restrepo, H., 1973. Geología de los cuadrángulos H-12 Bucaramanga y H-13 Pamplona. Boletín Geológico de Ingeominas 21, 1–132.
- Wasteneys, H.A., Clark, A.H., Farrar, E., Langridge, R.J., 1995. Grenvillian granulite facies metamorphism in the Arequipa Massif, Peru: a Laurentia-Gondwana link. Earth and Planetary Science Letters 132, 63–73.
- Wasteneys, H., Mclelland, J., Lumbers, S., 1999. Precise zircon geochronology in the Adirondacks Lowlands and implications for revising plate-tectonic models of the Central Metasedimentary belt and Adirondack Mountains, Grenville Province, Ontario and New York. Canadian Journal of Earth Sciences 36, 967–984.
- Weber, B., Hecht, L., 2003. Petrology and geochemistry of metaigneous rocks from a Grenvillian basement fragment in the Maya block: the Guichicovi complex, Oaxaca, southern Mexico. Precambrian Research 124, 41–67.
- Weber, B., Köhler, H., 1999. Sm–Nd, Rb–Sr and U–Pb geochronology of a Grenville Terrane in Southern Mexico: origin and geologic history of the Guichicovi Complex. Precambrian Research 96, 245–262.
- Wilson, J.J., Reyes, L., 1964. Geología del cuadrángulo de Pataz. Carta geológica Nacional, 91p.
- Yañez, P., Ruiz, J., Patchett, J.P., Ortega-Gutiérrez, F., Gehrels, G., 1991. Isotopic studies of the Acatlan Complex, southern Mexico: Implications for Paleozoic North American tectonics. Geological Society of America Bulletin 103, 817–828.